Mechanical Systems and Signal Processing 22 (2008) 1751–1773

Contents lists available at ScienceDirect

Mechanical Systems and Signal Processing

journal homepage: www.elsevier.com/locate/jnlabr/ymssp

Perturbation methods for the estimation of parameter variability in stochastic model updating

Hamed Haddad Khodaparast [a], John E. Mottershead [a,*], Michael I. Friswell [b]

[a] Department of Engineering, University of Liverpool, Brownlow Hill, Liverpool L69 3GH, UK
[b] Department of Aerospace Engineering, University of Bristol, Queens Building, University Walk, Bristol BS8 1TR, UK

ARTICLE INFO

Article history:
Received 22 November 2007
Received in revised form
29 February 2008
Accepted 4 March 2008
Available online 8 March 2008

Keywords:
Parameter variability
Model updating

ABSTRACT

The problem of model updating in the presence of test-structure variability is addressed. Model updating equations are developed using the sensitivity method and presented in a stochastic form with terms that each consist of a deterministic part and a random variable. Two perturbation methods are then developed for the estimation of the first and second statistical moments of randomised updating parameters from measured variability in modal responses (e.g. natural frequencies and mode shapes). A particular aspect of the stochastic model updating problem is the requirement for large amounts of computing time, which may be reduced by making various assumptions and simplifications. It is shown that when the correlation between the updating parameters and the measurements is omitted, then the requirement to calculate the second-order sensitivities is no longer necessary, yet there is no significant deterioration in the estimated parameter distributions. Numerical simulations and a physical experiment are used to illustrate the stochastic model updating procedure.

1. Introduction

The deterministic finite-element model updating problem [1,2] is well established, both in the development of methods and in application to industrial-scale structures. The stochastic model updating problem includes not only the variability in measurement signals due to noise, but also the variability that exists between nominally identical test structures, built in the same way from the same materials but with manufacturing and material variability [3,4]. Similar variability is know to result from environmental erosion, damage [5–7], or disassembly and reassembly of the same structure [8].

The propagation of uncertain parameters in finite-element models [9] has been carried out frequently but is of limited value when the uncertain parameters cannot be measured, typically damping and stiffness terms in mechanical joints or material-property variability. What can be measured is the variability in dynamic behaviour as represented by natural frequencies, mode-shapes, or frequency response functions. Then the inverse problem becomes one of inferring the parameter uncertainty from statistical measured data. This leads to improved confidence in the updated parameters of the finite-element model.

Statistical methods for the treatment of measurement noise in model updating were established in 1974 by Collins et al. [10] and more recently by Friswell [11]. In these approaches, the randomness arises only from the measurement noise and the updating parameters take unique values, to be found by iterative correction to the estimated means, whilst the variances are minimised. Mares et al. [3] adapted the method of Collins et al. [10] within a gradient-regression formulation

* Corresponding author. Tel.: +44 151 794 4827; fax: +44 151 794 4848.
E-mail address: j.e.mottershead@liverpool.ac.uk (J.E. Mottershead).

0888-3270/$ - see front matter
doi:10.1016/j.ymssp.2008.03.001

for the treatment of test-structure variability. Distributions of finite-element predictions were made to converge upon measured vibration response distributions, with the result that the means and standard deviations of the updating parameters were determined. Other statistical approaches that have been applied in model updating include Bayesian methods (Beck and Katafygiotis [12,13], Kershchen et al. [14], Mares et al. [15]) and the maximum likelihood method proposed by Fonseca et al. [16].

The use of randomised updating parameters leads inevitably to increased computation and therefore there is interest in developing efficient solutions. The perturbation approach is promising in this regard although its range of application is limited to small uncertainties. This restriction is in fact similar to the restriction on conventional deterministic model updating, that the initial starting estimate should be close to the true value. Both versions of the updating method, deterministic and stochastic, are applied iteratively so that the restriction applies step-by-step. Also the data should be sensitive to the updating parameters, so that only small changes are encountered. A recent paper by Hua et al. [7] addresses the problem of test-structure variability by a perturbation method. The predicted mean values and the matrix of predicted covariances are converged upon measured values and in so doing the first two statistical moments of the uncertain updating parameters are determined. The method is applicable to the problem of test-structure variability whereas the methods described by Collins et al. [10] and Friswell [11], both minimum variance estimators, are not. However, the method of Hua et al. [7] requires the determination of second-order sensitivities, which is an expensive computation.

In the present article a new method, based upon the perturbation procedure, is developed in two versions. In the first version of the method, the correlation between the updated parameters and measured data is omitted. This results in a procedure that requires only the first-order matrix of sensitivities. The second procedure includes this correlation (after the first iteration) but is a more expensive computation requiring the second-order sensitivities. It is shown in numerical simulations that the first method produces results that are equally acceptable as those produced by the second method or by Hua's approach [7]. The article includes a discussion of different forward propagation methods (including mean-centred first-order perturbation, the asymptotic integral [17,18], and Monte-Carlo simulation) used to evaluate certain covariance matrices as part of the updating procedure. Issues of sample size and regularisation of the ill-conditional stochastic model updating equations are considered. A series of simulated case studies are presented and finally the first version of the method is applied to the problem of determining thickness variability in a collection of plates from measured natural frequencies. Gaussian distributions are used in the simulated and experimental examples, but the method is not restricted to Gaussian distributions in either the variability of samples or in measurement noise. The validity of the updated finite-element model [19] is assessed using measured higher natural frequency distributions beyond the set of distributions used for updating the first and second statistical moments of the parameters.

2. The perturbation method

According to the conventional, deterministic model updating method an estimate $\boldsymbol{\theta}_{j+1}$ may be updated by using a prior estimate $\boldsymbol{\theta}_j$ as

$$\boldsymbol{\theta}_{j+1} = \boldsymbol{\theta}_j + \mathbf{T}_j(\mathbf{z}_m - \mathbf{z}_j) \tag{1}$$

where $\mathbf{z}_j \in \Re^{n\times 1}$ is the vector of estimated output parameters (e.g. eigenvalues and eigenvectors), $\mathbf{z}_m \in \Re^{n\times 1}$ is the vector of measured data, $\boldsymbol{\theta} \in \Re^{m\times 1}$ is the vector of system parameters and $\mathbf{T}_j$ is a transformation matrix. In order to take into account the variability in measurements arising from multiple sources, including manufacturing tolerances in nominally identical test structures as well as measurement noise, the modal parameters are represented as

$$\mathbf{z}_m = \overline{\mathbf{z}}_m + \Delta\mathbf{z}_m \tag{2}$$

$$\mathbf{z}_j = \overline{\mathbf{z}}_j + \Delta\mathbf{z}_j \tag{3}$$

where the overbar denotes mean values and $\Delta\mathbf{z}_m, \Delta\mathbf{z}_j \in \Re^{n\times 1}$ are vectors of random variables.

The hyperellipses represented by $\{\overline{\mathbf{z}}_m, \mathrm{Cov}(\mathbf{z}_m, \mathbf{z}_m)\}$ and $\{\overline{\mathbf{z}}_j, \mathrm{Cov}(\mathbf{z}_j, \mathbf{z}_j)\}$ define the space of measurements and predictions, respectively.

Correspondingly, we define the variability in physical parameters at the jth iteration as

$$\boldsymbol{\theta}_j = \overline{\boldsymbol{\theta}}_j + \Delta\boldsymbol{\theta}_j \tag{4}$$

and now cast the stochastic model updating problem as,

$$\overline{\boldsymbol{\theta}}_{j+1} + \Delta\boldsymbol{\theta}_{j+1} = \overline{\boldsymbol{\theta}}_j + \Delta\boldsymbol{\theta}_j + (\overline{\mathbf{T}}_j + \Delta\mathbf{T}_j)(\overline{\mathbf{z}}_m + \Delta\mathbf{z}_m - \overline{\mathbf{z}}_j - \Delta\mathbf{z}_j) \tag{5}$$

where the transformation matrix becomes,

$$\mathbf{T}_j = \overline{\mathbf{T}}_j + \Delta\mathbf{T}_j \tag{6}$$

$$\Delta\mathbf{T}_j = \sum_{k=1}^{n} \frac{\partial\overline{\mathbf{T}}_j}{\partial z_{mk}} \Delta z_{mk} \tag{7}$$

In the above equations, $\overline{\mathbf{T}}_j$ denotes the transformation matrix at the parameter means, $\overline{\mathbf{T}}_j = \mathbf{T}(\overline{\boldsymbol{\theta}}_j)$, and Δz_{mk} denotes the kth element of $\Delta\mathbf{z}_m$. We seek the parameterisation, $\overline{\boldsymbol{\theta}}_{j+1} + \Delta\boldsymbol{\theta}_{j+1}$, that converges the prediction space, $\overline{\mathbf{z}}_{j+1} + \Delta\mathbf{z}_{j+1}$, upon the measurement space $\overline{\mathbf{z}}_m + \Delta\mathbf{z}_m$. Consequently, $\mathbf{T}_j$ becomes a function of measured variability $\Delta\mathbf{z}_m$ according to Eqs. (6) and (7), since the updated parameters are determined at each iteration by converging the model predictions upon the measurements.

Application of the perturbation method, by separating the zeroth-order and first-order terms from Eq. (5), leads to,

$$\mathbf{O}(\Delta^0): \quad \overline{\boldsymbol{\theta}}_{j+\mathbf{1}} = \overline{\boldsymbol{\theta}}_j + \overline{\mathbf{T}}_j(\overline{\mathbf{z}}_m - \overline{\mathbf{z}}_j) \tag{8}$$

$$\mathbf{O}(\Delta^1): \quad \Delta\boldsymbol{\theta}_{j+\mathbf{1}} = \Delta\boldsymbol{\theta}_j + \overline{\mathbf{T}}_j(\Delta\mathbf{z}_m - \Delta\mathbf{z}_j) + \left(\left(\sum_{k=1}^{n} \frac{\partial \overline{\mathbf{T}}_j}{\partial z_{mk}} \Delta z_{mk}\right)(\overline{\mathbf{z}}_m - \overline{\mathbf{z}}_j)\right) \tag{9}$$

Eq. (8) gives the estimate of the parameter means and Eq. (9) is used in determining the parameter covariance matrix.

It will be seen that Eqs. (8) and (9) are different from the equations developed by Hua et al. [7] using an apparently similar approach. This difference arises because Hua et al. [7] expand $\mathbf{z}_m$, $\mathbf{z}_j$ and $\Delta\boldsymbol{\theta}_j$ in terms of Δz_{mk} (just as we expanded $\mathbf{T}_j$ in Eqs. (6) and (7)) before applying the perturbation method. Also, Hua et al. [7] worked in terms of the sensitivity matrix $\mathbf{S}_j$ rather than the matrix $\mathbf{T}_j$ used in the present analysis. Both approaches are perfectly acceptable but the method described in Ref. [7] does not contain an equivalent to the second right-hand-side term, $\overline{\mathbf{T}}_j(\Delta\mathbf{z}_m - \Delta\mathbf{z}_j)$. We will see in what follows that the presence of this term leads to significant advantages not available to users of the method by Hua et al. [7].

Changing the position of variable Δz_{mk} and the vector $(\overline{\mathbf{z}}_m - \overline{\mathbf{z}}_j)$ in Eq. (9) leads to the expression,

$$\Delta\boldsymbol{\theta}_{j+1} = \Delta\boldsymbol{\theta}_j + \left[\frac{\partial \overline{\mathbf{T}}_j}{\partial z_{m1}}(\overline{\mathbf{z}}_m - \overline{\mathbf{z}}_j) \; \frac{\partial \overline{\mathbf{T}}_j}{\partial z_{m2}}(\overline{\mathbf{z}}_m - \overline{\mathbf{z}}_j) \; \cdots \; \frac{\partial \overline{\mathbf{T}}_j}{\partial z_{mn}}(\overline{\mathbf{z}}_m - \overline{\mathbf{z}}_j)\right]\Delta\mathbf{z}_m + \overline{\mathbf{T}}_j(\Delta\mathbf{z}_m - \Delta\mathbf{z}_j) \tag{10}$$

or,

$$\Delta\boldsymbol{\theta}_{j+1} = \Delta\boldsymbol{\theta}_j + \mathbf{A}_j\,\Delta\mathbf{z}_m + \overline{\mathbf{T}}_j(\Delta\mathbf{z}_m - \Delta\mathbf{z}_j) \tag{11}$$

where the deterministic matrix,

$$\left[\frac{\partial \overline{\mathbf{T}}_j}{\partial z_{m1}}(\overline{\mathbf{z}}_m - \overline{\mathbf{z}}_j) \; \frac{\partial \overline{\mathbf{T}}_j}{\partial z_{m2}}(\overline{\mathbf{z}}_m - \overline{\mathbf{z}}_j) \; \cdots \; \frac{\partial \overline{\mathbf{T}}_j}{\partial z_{mn}}(\overline{\mathbf{z}}_m - \overline{\mathbf{z}}_j)\right]$$

is now replaced by the matrix $\mathbf{A}_j$. The matrix $(\partial\overline{\mathbf{T}}_j/\partial z_{mk})$ is deterministic since it is evaluated at the means of measured system responses $(z_{mk} = \overline{z}_{mk})$.

It now becomes apparent, from Eq. (11) that the parameter covariance matrix can be found at j+1th iteration as,

$$\begin{aligned}
&\mathrm{Cov}(\Delta\boldsymbol{\theta}_{j+1}, \Delta\boldsymbol{\theta}_{j+1}) = \mathrm{Cov}(\Delta\boldsymbol{\theta}_j + \mathbf{A}_j\Delta\mathbf{z}_m + \overline{\mathbf{T}}_j(\Delta\mathbf{z}_m - \Delta\mathbf{z}_j), \Delta\boldsymbol{\theta}_j + \mathbf{A}_j\Delta\mathbf{z}_m + \overline{\mathbf{T}}_j(\Delta\mathbf{z}_m - \Delta\mathbf{z}_j))\\
&\quad = \mathrm{Cov}(\Delta\boldsymbol{\theta}_j, \Delta\boldsymbol{\theta}_j) + \mathrm{Cov}(\Delta\boldsymbol{\theta}_j, \Delta\mathbf{z}_m)\mathbf{A}_j^T + \mathrm{Cov}(\Delta\boldsymbol{\theta}_j, \Delta\mathbf{z}_m)\overline{\mathbf{T}}_j^T - \mathrm{Cov}(\Delta\boldsymbol{\theta}_j, \Delta\mathbf{z}_j)\overline{\mathbf{T}}_j^T\\
&\qquad + (\mathrm{Cov}(\Delta\boldsymbol{\theta}_j, \Delta\mathbf{z}_m)\mathbf{A}_j^T)^T + \mathbf{A}_j\,\mathrm{Cov}(\Delta\mathbf{z}_m, \Delta\mathbf{z}_m)\mathbf{A}_j^T + \mathbf{A}_j\,\mathrm{Cov}(\Delta\mathbf{z}_m, \Delta\mathbf{z}_m)\overline{\mathbf{T}}_j^T - \mathbf{A}_j\,\mathrm{Cov}(\Delta\mathbf{z}_m, \Delta\mathbf{z}_j)\overline{\mathbf{T}}_j^T\\
&\qquad + (\mathrm{Cov}(\Delta\boldsymbol{\theta}_j, \Delta\mathbf{z}_m)\overline{\mathbf{T}}_j^T)^T + (\mathbf{A}_j\mathrm{Cov}(\Delta\mathbf{z}_m, \Delta\mathbf{z}_m)\overline{\mathbf{T}}_j^T)^T + \overline{\mathbf{T}}_j\,\mathrm{Cov}(\Delta\mathbf{z}_m, \Delta\mathbf{z}_m)\overline{\mathbf{T}}_j^T - \overline{\mathbf{T}}_j\,\mathrm{Cov}(\Delta\mathbf{z}_m, \Delta\mathbf{z}_j)\overline{\mathbf{T}}_j^T\\
&\qquad - (\mathrm{Cov}(\Delta\boldsymbol{\theta}_j, \Delta\mathbf{z}_j)\overline{\mathbf{T}}_j^T)^T - (\mathbf{A}_j\,\mathrm{Cov}(\Delta\mathbf{z}_m, \Delta\mathbf{z}_j)\overline{\mathbf{T}}_j^T)^T - (\overline{\mathbf{T}}_j\,\mathrm{Cov}(\Delta\mathbf{z}_m, \Delta\mathbf{z}_j)\overline{\mathbf{T}}_j^T)^T + \overline{\mathbf{T}}_j\,\mathrm{Cov}(\Delta\mathbf{z}_j, \Delta\mathbf{z}_j)\overline{\mathbf{T}}_j^T
\end{aligned} \tag{12}$$

A common assumption, that originated with the 1974 paper of Collins et al. [10], is to omit the correlation between the measurement, $\mathbf{z}_m$, and the system parameters, $\boldsymbol{\theta}_j$. Friswell [11] corrected this omission by including the correlation after the first iteration. In this paper we consider the effect of the omitted correlation on the converged prediction space using the formulation described above.

When the measurements and parameters are assumed to be uncorrelated, then $\mathrm{Cov}(\Delta\mathbf{z}_m, \Delta\boldsymbol{\theta}_j) = \mathbf{0}$ and also $\mathrm{Cov}(\Delta\mathbf{z}_m, \Delta\mathbf{z}_j) = \mathbf{0}$. It will be shown later that the matrix $\mathbf{A}_j$ vanishes under the same assumption. Consequently, Eq. (12) simplifies to give,

$$\begin{aligned}
\mathrm{Cov}(\Delta\boldsymbol{\theta}_{j+1}, \Delta\boldsymbol{\theta}_{j+1}) = {} & \mathrm{Cov}(\Delta\boldsymbol{\theta}_j, \Delta\boldsymbol{\theta}_j) - \mathrm{Cov}(\Delta\boldsymbol{\theta}_j, \Delta\mathbf{z}_j)\overline{\mathbf{T}}_j^T + \overline{\mathbf{T}}_j\,\mathrm{Cov}(\Delta\mathbf{z}_m, \Delta\mathbf{z}_m)\overline{\mathbf{T}}_j^T - \overline{\mathbf{T}}_j\mathrm{Cov}(\Delta\mathbf{z}_j, \Delta\boldsymbol{\theta}_j)\\
& + \overline{\mathbf{T}}_j\mathrm{Cov}(\Delta\mathbf{z}_j, \Delta\mathbf{z}_j)\overline{\mathbf{T}}_j^T
\end{aligned} \tag{13}$$

Eq. (13) does not include the second-order sensitivity matrix. This leads to very considerable reduction in computational effort, of great practical value in engineering applications if the $\mathrm{Cov}(\Delta\mathbf{z}_m, \Delta\boldsymbol{\theta}_j) = \mathbf{0}$ assumption is shown to be viable. Under this assumption model updating is carried out using the two recursive Eqs. (8) and (13). The transformation matrix may be expressed as the weighted pseudo inverse, which is analogous to the transformation used in deterministic model updating [1,2]. To the zeroth order of smallness the same equation applies,

$$\overline{\mathbf{T}}_j = (\overline{\mathbf{S}}_j^T\mathbf{W}_1\overline{\mathbf{S}}_j + \mathbf{W}_2)^{-1}\overline{\mathbf{S}}_j^T\mathbf{W}_1 \tag{14}$$

In Eq. (14), $\overline{\mathbf{S}}_j$ denotes the sensitivity matrix at the parameter means, $\overline{\mathbf{S}}_j = \mathbf{S}(\overline{\boldsymbol{\theta}}_j)$, and the choice of $\mathbf{W}_1 = \mathbf{I}$ and $\mathbf{W}_2 = \mathbf{0}$ results in the pseudo inverse. In the case of ill-conditioned model-updating equations, the minimum-norm regularised solution is obtained when $\mathbf{W}_2 = \lambda \mathbf{I}$ and λ is the regularisation parameter that locates the corner of the L-curve obtained by plotting the norms $||\bar{\boldsymbol{\theta}}_{j+1} - \bar{\boldsymbol{\theta}}_j|| \text{vs} ||\bar{\mathbf{S}}_j(\bar{\boldsymbol{\theta}}_{j+1} - \bar{\boldsymbol{\theta}}_j) - (\bar{\mathbf{z}}_m - \bar{\mathbf{z}}_j)||$ as λ is varied [20].

The above procedure may be implemented in the following steps:

1. Determine the mean vector and covariance matrix of the measured data $(\bar{\mathbf{z}}_m, \mathrm{Cov}(\mathbf{z}_m, \mathbf{z}_m))$ and set $j = 0$.
2. Initialise the means and standard deviations of the system parameters.
3. Determine the mean value of the analytical output parameters, $\bar{\mathbf{z}}_j$, and the covariance matrices,$\mathrm{Cov}(\Delta\boldsymbol{\theta}_j, \Delta\mathbf{z}_j)$ and $\mathrm{Cov}(\Delta\mathbf{z}_j, \Delta\mathbf{z}_j)$, using a forward propagation method such as perturbation, the asymptotic integral or Monte-Carlo simulation.
4. Calculate the sensitivity matrix $\bar{\mathbf{S}}_j$ at the current mean values of system parameters, choose suitable weighting matrices for regularisation and determine the transformation matrix $\bar{\mathbf{T}}_j$ according to Eq. (14).
5. Update the mean values and covariance matrix of the system parameters using Eqs. (8) and (13), respectively.
6. If both the means and standard deviations of the parameters have converged go to step (7); otherwise set $j = j$+1, go to step (3).
7. Stop.

If the correlation between the parameters and measurements is included, then $\mathrm{Cov}(\Delta\boldsymbol{\theta}_j, \Delta\mathbf{z}_m)$ and matrix $\mathbf{A}_j$ must be updated as follows,

$$\begin{aligned}\mathrm{Cov}(\Delta\boldsymbol{\theta}_{j+1}, \Delta\mathbf{z}_m) &= \mathrm{Cov}(\Delta\boldsymbol{\theta}_j + \mathbf{A}_j\,\Delta\mathbf{z}_m + \bar{\mathbf{T}}_j(\Delta\mathbf{z}_m - \Delta\mathbf{z}_j), \Delta\mathbf{z}_m)\\ &= \mathrm{Cov}(\Delta\boldsymbol{\theta}_j, \Delta\mathbf{z}_m) + (\mathbf{A}_j + \bar{\mathbf{T}}_j)\,\mathrm{Cov}(\Delta\mathbf{z}_m, \Delta\mathbf{z}_m) - \bar{\mathbf{T}}_j\,\mathrm{Cov}(\Delta\mathbf{z}_j, \Delta\mathbf{z}_m)\end{aligned} \tag{15}$$

The matrix $\mathbf{A}_{j+1}$ is determined from

$$\mathbf{A}_{j+1} = \left[\left.\frac{\partial \bar{\mathbf{T}}_{j+1}}{\partial z_{m1}}\right|_{z_{m1}=\bar{z}_{m1}} (\bar{\mathbf{z}}_m - \bar{\mathbf{z}}_{j+1}) \quad \left.\frac{\partial \bar{\mathbf{T}}_{j+1}}{\partial z_{m2}}\right|_{z_{m2}=\bar{z}_{m2}} (\bar{\mathbf{z}}_m - \bar{\mathbf{z}}_{j+1}) \quad \cdots \quad \left.\frac{\partial \bar{\mathbf{T}}_{j+1}}{\partial z_{mn}}\right|_{z_{mn}=\bar{z}_{mn}} (\bar{\mathbf{z}}_m - \bar{\mathbf{z}}_{j+1}) \right] \tag{16}$$

where

$$\left.\frac{\partial \bar{\mathbf{T}}_{j+1}}{\partial z_{mk}}\right|_{z_{mk}=\bar{z}_{mk}} = \sum_{i=1}^{m} \frac{\partial \bar{\mathbf{T}}_{j+1}}{\partial \bar{\theta}_{(j+1),i}} \left.\frac{\partial \bar{\theta}_{(j+1),i}}{\partial z_{mk}}\right|_{z_{mk}=\bar{z}_{mk}}; \quad k = 1, 2, \ldots, n \tag{17}$$

$$\begin{aligned}\frac{\partial \bar{\mathbf{T}}_{j+1}}{\partial \theta_{(j+1),i}} = {} & (\bar{\mathbf{S}}_{j+1}^{\mathrm{T}} \mathbf{W}_1 \bar{\mathbf{S}}_{j+1} + \mathbf{W}_2)^{-1} \frac{\partial \bar{\mathbf{S}}_{j+1}^{\mathrm{T}}}{\partial \theta_{(j+1),i}} \mathbf{W}_1 - (\bar{\mathbf{S}}_{j+1}^{\mathrm{T}} \mathbf{W}_1 \bar{\mathbf{S}}_{j+1} + \mathbf{W}_2)^{-1} \left(\frac{\partial \bar{\mathbf{S}}_{j+1}^{\mathrm{T}}}{\partial \theta_{(j+1),i}} \mathbf{W}_1 \bar{\mathbf{S}}_{j+1} + \bar{\mathbf{S}}_{j+1}^{\mathrm{T}} \mathbf{W}_1 \frac{\partial \bar{\mathbf{S}}_{j+1}}{\partial \bar{\theta}_{(j+1),i}} \right)\\ & \times (\bar{\mathbf{S}}_{j+1}^{\mathrm{T}} \mathbf{W}_1 \bar{\mathbf{S}}_{j+1} + \mathbf{W}_2)^{-1} \bar{\mathbf{S}}_{j+1}^{\mathrm{T}} \mathbf{W}_1\end{aligned} \tag{18}$$

and,

$$\frac{\partial \bar{\boldsymbol{\theta}}_{j+1}}{\partial z_{mk}} = \frac{\partial \bar{\boldsymbol{\theta}}_j}{\partial z_{mk}} + \bar{\mathbf{T}}_j \left(\frac{\partial \bar{\mathbf{z}}_m}{\partial z_{mk}} - \frac{\partial \bar{\mathbf{z}}_j}{\partial z_{mk}} \right) + \frac{\partial \bar{\mathbf{T}}_j}{\partial z_{mk}} (\bar{\mathbf{z}}_m - \bar{\mathbf{z}}_j) \tag{19}$$

The terms of $(\partial \bar{\mathbf{z}}_m / \partial z_{mk})|_{z_{mk}=\bar{z}_{mk}}$ are given by

$$\left.\frac{\partial \bar{z}_{mj}}{\partial z_{mk}}\right|_{z_{mk}=\bar{z}_{mk}} = \begin{cases} 1 & \text{if } j = k \\ 0 & \text{if } j \neq k \end{cases} \tag{20}$$

and from the chain rule,

$$\frac{\partial \bar{\mathbf{z}}_j}{\partial z_{mk}} = \bar{\mathbf{S}}_j \frac{\partial \bar{\boldsymbol{\theta}}_j}{\partial z_{mk}} \tag{21}$$

Hence, a system of four recursive Eqs. (8), (12), (15) and (19) are required to determine the means and co-variance matrix of the parameters.

By the analysis above it is seen that the parameter covariances $\mathrm{Cov}(\Delta\boldsymbol{\theta}_{j+1}, \Delta\boldsymbol{\theta}_{j+1})$ are expressed in terms of the measured output covariance matrix $\mathrm{Cov}(\Delta\mathbf{z}_m, \Delta\mathbf{z}_m)$ together with the covariances $\mathrm{Cov}(\Delta\boldsymbol{\theta}_j, \Delta\mathbf{z}_j), \mathrm{Cov}(\Delta\mathbf{z}_j, \Delta\mathbf{z}_j)$ and in the case of Eq. (13) in terms of $\mathrm{Cov}(\Delta\boldsymbol{\theta}_j, \Delta\mathbf{z}_m)$, which is updated using Eq. (15). The derivatives $(\partial \bar{\mathbf{T}}_j / \partial z_{mk})$, $(\partial \mathbf{z}_j / \partial z_{mk})$ and matrix $\mathbf{A}_j$ are found by using Eqs. (17), (21) and (16), respectively, and

$$\mathrm{Cov}(\Delta\mathbf{z}_j, \Delta\mathbf{z}_m) = \bar{\mathbf{S}}_j\,\mathrm{Cov}(\Delta\boldsymbol{\theta}_j, \Delta\mathbf{z}_m) \tag{22}$$

This procedure may be implemented according the following steps:

1. Determine the mean vector and covariance matrix of the measured data $(\bar{\mathbf{z}}_m, \mathrm{Cov}(\mathbf{z}_m, \mathbf{z}_m))$ and set $j = 0$.
2. Initialise the means and standard deviations of the system parameters.

3. Initialise $\mathrm{Cov}(\Delta\boldsymbol{\theta}_j, \Delta\mathbf{z}_m)$ and $(\partial\bar{\boldsymbol{\theta}}_j/\partial z_{mk})$ to zero—consequently matrix $\mathbf{A}_j$ and $\mathrm{Cov}(\Delta\mathbf{z}_j, \Delta\mathbf{z}_m)$ are zero (Eqs. (16), (17) and (22)).
4. Determine the mean value of the analytical output parameters, $\bar{\mathbf{z}}_j$, and the covariance matrices, $\mathrm{Cov}(\Delta\boldsymbol{\theta}_j, \Delta\mathbf{z}_j)$ and $\mathrm{Cov}(\Delta\mathbf{z}_j, \Delta\mathbf{z}_j)$, using a forward propagation method such as perturbation, the asymptotic integral or Monte-Carlo simulation.
5. Calculate the sensitivity matrix $\bar{\mathbf{S}}_j$ at the current mean value of system parameters and choose suitable weighting matrices for regularisation in order to compute the transformation matrix introduced in Eq. (14).
6. Update the mean values and covariance matrix of the system parameters using Eqs. (8) and (12), respectively.
7. Update $\mathrm{Cov}(\Delta\boldsymbol{\theta}_j, \Delta\mathbf{z}_m)$ and $(\partial\bar{\boldsymbol{\theta}}_j/\partial z_{mk})$ using Eqs. (15) and (19), then update $\mathbf{A}_j$ using Eqs. (16), (17) and (18) and $\mathrm{Cov}(\Delta\mathbf{z}_j, \Delta\mathbf{z}_m)$ using Eq. (22).
8. If both the mean values of the parameters and their standard deviations have converged go to step (9); otherwise set $j = j+1$, go to step (4).
9. Stop.

The covariance matrices $\mathrm{Cov}(\Delta\boldsymbol{\theta}_j, \Delta\mathbf{z}_j)$ and $\mathrm{Cov}(\Delta\mathbf{z}_j, \Delta\mathbf{z}_j)$ may be evaluated by forward propagation using a variety of techniques including mean-centred first-order perturbation, the asymptotic integral and Monte-Carlo simulation as will be explained in the following section.

3. Evaluation of covariance matrices by forward propagation

In this section, the subscript j and prefix Δ on $\Delta\boldsymbol{\theta}$ and $\Delta\mathbf{z}$ is omitted for reasons of simplicity. The system parameters are assumed to follow a chosen multivariate probability density function. Unless knowledge exists to contrary this will in practice be a Gaussian density function expressed as,

$$\boldsymbol{\theta} \in N_n(\bar{\boldsymbol{\theta}}, \mathrm{Cov}(\boldsymbol{\theta}, \boldsymbol{\theta})) \tag{23}$$

3.1. Mean-centred first-order perturbation

The output vector, $\mathbf{z}$, is expanded about the mean value $\mathbf{z}(\bar{\boldsymbol{\theta}})$ as,

$$\mathbf{z} = \mathbf{z}(\bar{\boldsymbol{\theta}}) + \sum_{i=1}^{m} \left.\frac{\partial \mathbf{z}}{\partial \theta_i}\right|_{\theta_i=\bar{\theta}_i} (\theta_i - \bar{\theta}_i) + \sum_{i=1}^{m}\sum_{j=1}^{m} \left.\frac{\partial^2 \mathbf{z}}{\partial \theta_i \partial \theta_j}\right|_{\substack{\theta_i = \bar{\theta}_i \\ \theta_j = \bar{\theta}_j}} (\theta_i - \bar{\theta}_i)(\theta_j - \bar{\theta}_j) + \cdots \tag{24}$$

and by truncating after the first-order term,

$$\mathbf{z} = \mathbf{z}(\bar{\boldsymbol{\theta}}) + \bar{\mathbf{S}}(\boldsymbol{\theta} - \bar{\boldsymbol{\theta}}) \Rightarrow \Delta\mathbf{z} = \bar{\mathbf{S}}\,\Delta\boldsymbol{\theta} \tag{25}$$

Therefore,

$$\bar{\mathbf{z}} \approx \mathbf{z}(\bar{\boldsymbol{\theta}}) \tag{26}$$

$$\mathrm{Cov}(\mathbf{z}, \mathbf{z}) = \bar{\mathbf{S}}\,\mathrm{Cov}(\boldsymbol{\theta}, \boldsymbol{\theta})\bar{\mathbf{S}}^T \tag{27}$$

$$\mathrm{Cov}(\boldsymbol{\theta}, \mathbf{z}) = \mathrm{Cov}(\boldsymbol{\theta}, \boldsymbol{\theta})\bar{\mathbf{S}}^T \tag{28}$$

The perturbation propagation approach has been used widely for its tractability and computational time-saving [16]. But there are limitations in using this method, which works well when the uncertainties are small and parameter distribution is Gaussian [18]. The asymptotic integral may be used for evaluating of $\bar{\mathbf{z}}$, $\mathrm{Cov}(\boldsymbol{\theta}, \mathbf{z})$ and $\mathrm{Cov}(\mathbf{z}, \mathbf{z})$ when probability density of the uncertain parameters is not assumed Gaussian.

3.2. The asymptotic integral

In this section the integrals that define all the terms of $\mathrm{Cov}(\mathbf{z}, \mathbf{z})$ and $\mathrm{Cov}(\boldsymbol{\theta}, \mathbf{z})$ are obtained by an asymptotic approximation. In general we consider the multidimensional integral of the form,

$$\mathrm{J} = \int_{\Re^m} \exp(-f(\boldsymbol{\theta}))\,\mathrm{d}\theta_1\,\mathrm{d}\theta_2 \ldots \mathrm{d}\theta_m \tag{29}$$

where $f(\boldsymbol{\theta}) \in \Re$ is a smooth function of $\boldsymbol{\theta} \in \Re^m$, infinitely differentiable over the unbounded domain $\Re^m$ [17]. Adhikari and Friswell [18] approximated an integral of this type by applying Laplace's method of asymptotic expansion [21],

$$\mathrm{J} \approx (2\pi)^{m/2} \exp\{-f(\boldsymbol{\varphi})\}||\mathbf{D}_f(\boldsymbol{\varphi})||^{-1/2} \tag{30}$$

where $\mathbf{D}_f(\boldsymbol{\varphi})$ is the Hessian matrix of $f(\boldsymbol{\theta})$ at $\boldsymbol{\theta} = \boldsymbol{\varphi}$, defined as an optimal point at which $f(\boldsymbol{\theta})$ reaches its global minimum. The method is based on the assumption that the integral is maximised when $f(\boldsymbol{\theta})$ reaches this global minimum.

Evaluation of the integrals appearing in the covariances,

$$\mathrm{Cov}(z_i, z_k) = [\mathrm{E}(z_i(\boldsymbol{\theta})z_k(\boldsymbol{\theta})) - \mathrm{E}(z_i(\boldsymbol{\theta}))\mathrm{E}(z_k(\boldsymbol{\theta}))]; \quad i,k = 1,2,\ldots,n, \tag{31}$$

$$\mathrm{Cov}(\theta_i, z_k) = [\mathrm{E}(\theta_i z_k(\boldsymbol{\theta})) - \mu_i \mathrm{E}(z_k(\boldsymbol{\theta}))]; \quad i = 1,2,\ldots,m; \quad k = 1,2,\ldots,n \tag{32}$$

is described in Appendix.

3.3. Monte-Carlo simulation

In the Monte-Carlo process a large number of samples of uncertain parameters $\boldsymbol{\theta}$ is generated according to the assumed parameter probability density function and the respective response values, $\mathbf{z}$, are evaluated from FE analysis. The mean values of output vector from mathematical model, $\bar{\mathbf{z}}$, the covariances of system parameters and outputs,$\mathrm{Cov}(\boldsymbol{\theta}, \mathbf{z})$ and covariance matrix of output parameters, $\mathrm{Cov}(\mathbf{z}, \mathbf{z})$, can be directly evaluated from the scatter of responses and the system parameters that provide the input to the simulation. Monte-Carlo simulation is the most accurate method but is computationally expensive and can be extremely time consuming.

4. Case studies on the evaluation of covariance matrices

Two case studies are considered, a 3 degree-of-freedom mass–spring system and a finite-element beam model with three elements having uncertain elastic moduli. In both cases the covariance matrices obtained by mean-centred first-order perturbation and the asymptotic integral are compared to the covariance matrix obtained from Monte-Carlo simulation.

4.1. Case study 1: 3 Degree-of-freedom mass– spring system

The model shown in Fig. 1 has deterministic parameters,

$$m_i = 1.0\ \mathrm{kg} \quad (i = 1,2,3), \quad k_i = 1.0\ \mathrm{N/m} \quad (i = 3,4), \quad k_6 = 3.0\ \mathrm{N/m}$$

and also uncertain random parameters,

$$\boldsymbol{\theta} = [k_1, k_2, k_5]^T \in N_3(\bar{\boldsymbol{\theta}}, \Sigma^2_{\theta\theta})$$

where

$$\bar{\boldsymbol{\theta}} = [2 \quad 2 \quad 2]^T \quad \text{and} \quad \Sigma^2_{\theta\theta} = \mathrm{diag}[0.09 \quad 0.09 \quad 0.09]$$

and N_3 denotes the multivariate normal (Gaussian) distribution in three random variables.

The covariance matrix $\mathrm{Cov}(\mathbf{z}, \mathbf{z})$ being symmetric has six independent elements. The covariance matrix $\mathrm{Cov}(\boldsymbol{\theta}, \mathbf{z})$ has nine elements. Fig. 2 shows the errors obtained by using mean-centred first-order propagation and asymptotic approximation with respect to the results obtained by Monte-Carlo simulation. Generally, the errors are smaller when using the asymptotic integral.

4.2. Case study 2: Finite-element model of a cantilever beam

The beam, with a rectangular cross-section 25 mm × 5.5 mm and a length of 0.5 m, is modelled using 10 Euler–Bernoulli beam elements as shown in Fig. 3. The elastic moduli of elements 3, 7 and 10 are considered as random variables,

$$\boldsymbol{\theta} = [E_3, E_7, E_{10}]^T \in N_3(\bar{\boldsymbol{\theta}}, \Sigma^2_{\theta\theta})$$

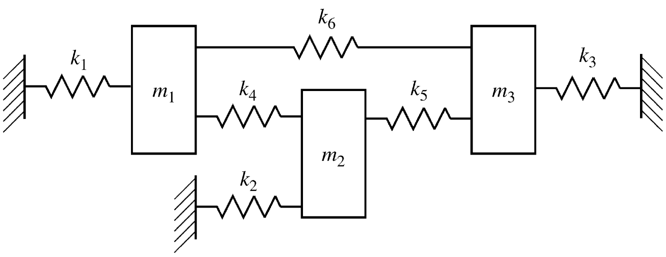

Fig. 1. Case study 1: 3 degree-of-freedom mass–spring system.

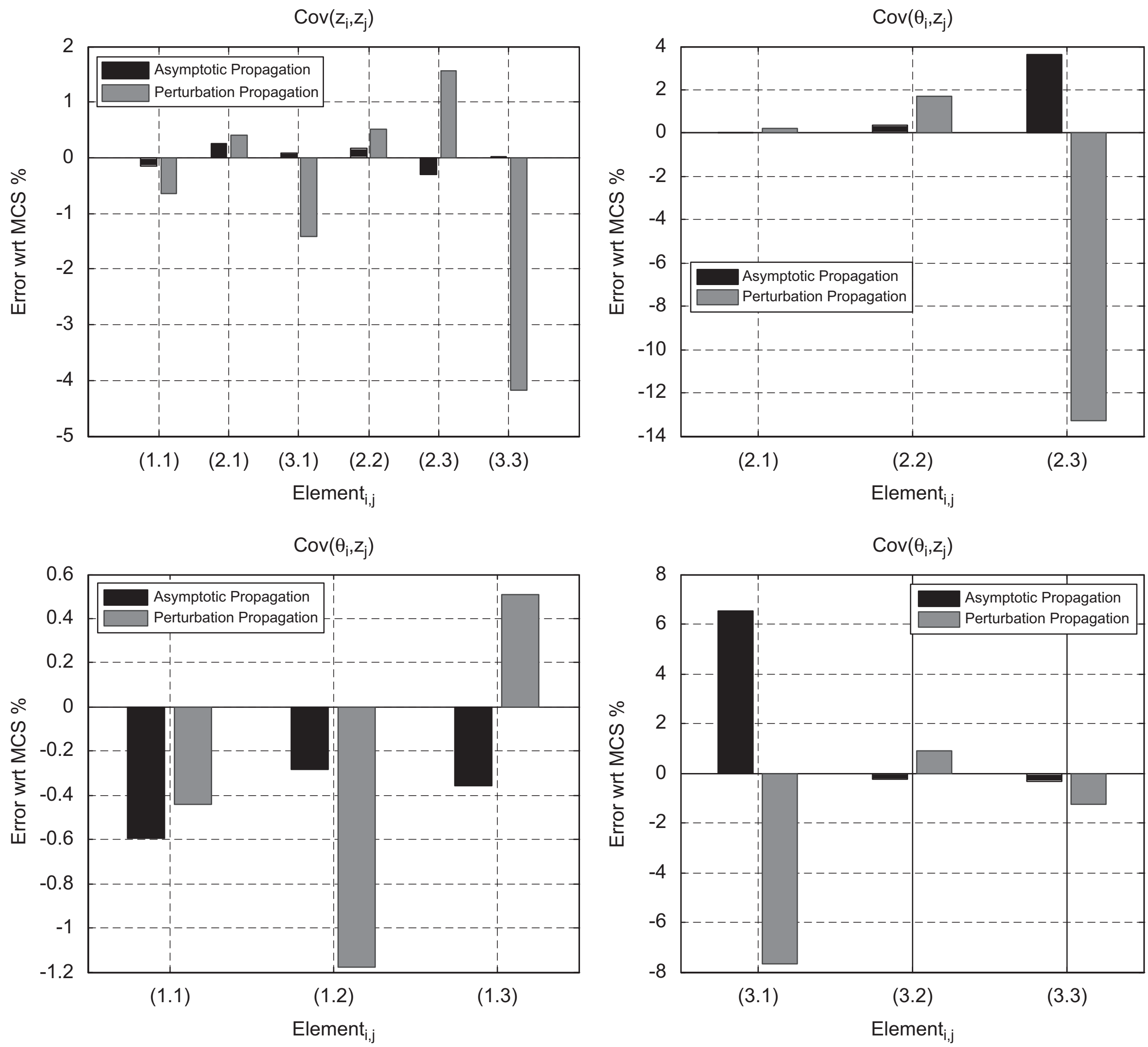

Fig. 2. Mass–spring system—estimation of Cov($\mathbf{z}, \mathbf{z}$)and Cov($\boldsymbol{\theta}, \mathbf{z}$).

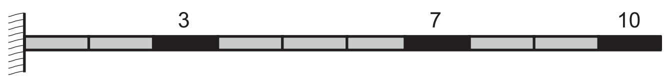

Fig. 3. Case study 2: cantilever beam.

where

$$\bar{\boldsymbol{\theta}} = [2.1 \times 10^{11} \quad 2.1 \times 10^{11} \quad 2.1 \times 10^{11}]^T \quad \text{and} \quad \Sigma^2_{\theta\theta} = \text{diag}[1 \times 10^{20} \quad 1 \times 10^{20} \quad 1 \times 10^{20}]$$

The errors in the estimated covariance matrices, with respect to Monte-Carlo simulation, are shown in Fig. 4. The errors in elements (3,1) and (3,2) of Cov($\boldsymbol{\theta}, \mathbf{z}$)appear larger than the others because the values of these terms are three orders of smallness less than the values of the other terms.

5. Numerical case studies on the identification of uncertainty

Two numerical case studies are used to illustrate the working of the perturbation methods, namely the 3 degree-of-freedom system described in Section 4 and also a finite-element pin-jointed truss structure. In addition to the present

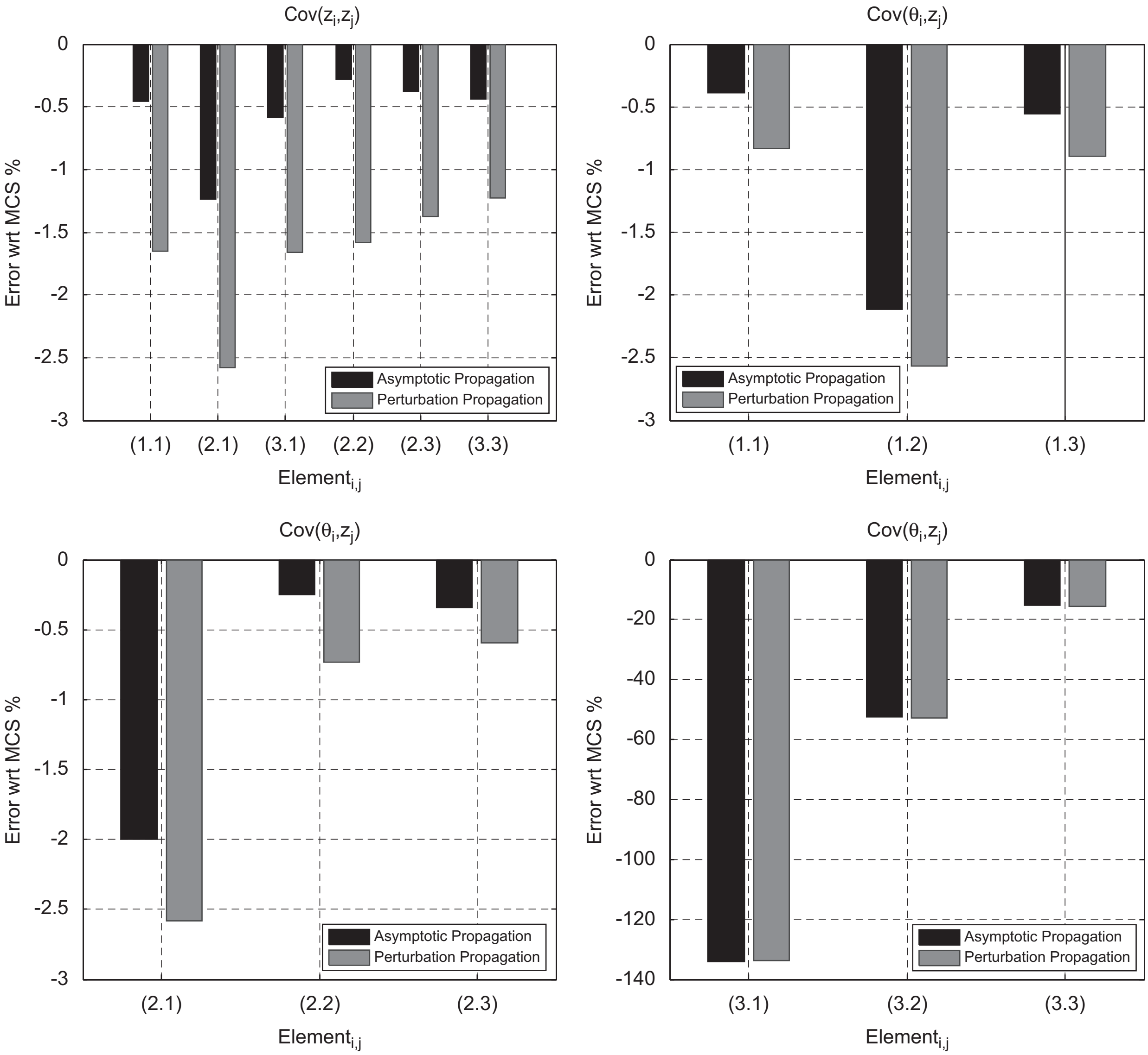

Fig. 4. Cantilever beam—estimation of $\mathrm{Cov}(\mathbf{z},\mathbf{z})$and $\mathrm{Cov}(\boldsymbol{\theta},\mathbf{z})$.

methodology, results obtained by using the minimum variance estimator of Collins et al. [10] and Friswell [11] are also presented.

5.1. Case study 1: 3 Degree-of-freedom mass–spring system

The simple example shown in Fig. 1 is considered, having known deterministic parameters,

$$m_i = 1.0\,\mathrm{kg} \quad (i = 1,2,3), \quad k_i = 1.0\,\mathrm{N/m} \quad (i = 3,4), \quad k_6 = 3.0\,\mathrm{N/m}$$

and the other parameters represented as unknown Gaussian random variables with mean values and standard deviations given by

$$\mu_{k_1} = 1.0\,\mathrm{N/m}, \quad \mu_{k_2} = 1.0\,\mathrm{N/m}, \quad \mu_{k_5} = 1.0\,\mathrm{N/m}$$

$$\sigma_{k1} = 0.20\,\mathrm{N/m}, \quad \sigma_{k2} = 0.20\,\mathrm{N/m}, \quad \sigma_{k5} = 0.20\,\mathrm{N/m}$$

The measured data, $\bar{\mathbf{z}}_m$ and $\mathrm{Cov}(\mathbf{z}_m,\mathbf{z}_m)$, are obtained by using Monte-Carlo simulation with 10,000 samples. This number of measurements is unrealistic but is used here to demonstrate the asymptotic properties of the methods. Later, the number of measurements will be varied to show the effect of this number on the parameter errors. The initial estimates of

Table 1
Updating results obtained by various methods (10,000 samples)

Parameters	Initial % error	% Error (1)	% Error (2)	% Error (3)	% Error (4)	% Error (5)
$\bar{k}_1$	100	1.20	1.32	1.21	1.62	17.43
$\bar{k}_2$	100	−2.43	−2.26	−2.18	−2.35	36.81
$\bar{k}_5$	100	0.71	0.57	0.23	1.86	58.20
S.D.(k_1)	50	0.31	0.88	−0.35	−89.80	−13.36
S.D.(k_2)	50	1.77	0.46	−1.27	−89.85	−12.07
S.D.(k_5)	50	1.96	0.24	−0.16	−90.20	−58.83

the unknown random parameters are

$$\overline{k}_1 = \overline{k}_2 = \overline{k}_5 = 2.0\ \mathrm{N/m}, \quad \mathrm{Cov}(k_i) = (0.3^2)\mathrm{N}^2/\mathrm{m}^2 \quad i = 1, 2, 5$$

so that a 100% initial error in mean values and a 50% initial error in standard deviations is represented.

Results obtained by the present perturbation methods ($\mathbf{W}_1 = \mathbf{I}, \mathbf{W}_2 = \mathbf{0}$), the method of Hua et al. [7], and the minimum variance estimators of Collins et al. [10] and Friswell [11] are shown in Table 1. The numbers, (1)–(5) in the table denote the following methods:

(1) The proposed method in which the correlation between measured data and system parameters is omitted (Eqs. (8) and (13)).
(2) The proposed method in which the correlation between measured data and system parameters is included after the first iteration (Eqs. (8), (12), (15) and (19)).
(3) Method introduced by Hua et al. [7].
(4) The minimum variance method of Collins et al. [10].
(5) The minimum variance method of Friswell [11].

It should be noted that the method of Hua et al. [7] does not require a starting estimate for the standard deviation of the unknown random parameters, which start from zero at the first iteration. In all cases forward propagation was carried out using Monte-Carlo simulation.

Firstly, it is seen that the results obtained by method (1), when the correlation of system parameters with the measured data is omitted, are at least as good as when this correlation is included. Methods (2) and (3) require the evaluation of the second-order sensitivity, which is an expensive computation and not needed when using method (1). Finally, it is seen that the minimum variance methods (4) and (5) are really not intended for the estimation of randomised parameters to represent test-piece variability. These methods work well when the variability is limited to measurement noise from a single test piece. Convergence of the parameter estimates by each of the different methods is shown in Figs. 5–9. It is seen from Fig. 8 that method (4) is slow to converge. Fig. 10 shows the convergence of the predictions upon experimental data in the space of the first three natural frequencies using method (1).

Ten thousand samples are clearly enough to obtain an accurate estimate of the parameter variability. Fig. 11 shows the convergence of the parameter standard deviations by method (1) as the number of samples is increased from 10 to 1000. In each case 10 runs of the updating algorithm were carried out to enable a range of solution errors to be determined. A different set of samples was used in each of the 10 runs. When only 10 samples were used errors were found in the range of 24–54%, while in the case of 1000 samples the errors ranged from 3% to 7%.

Figs. 12–14 show the convergence of the parameter statistics using only 10 samples with methods (1), (2) and (3). Converged results and percentage errors are given in Table 2. The 10 samples were different in each of the three cases, which are shown to converge to similar results. Figs. 15 and 16 show the convergence of scatter of predictions upon the scatter of simulated measurements in the planes of the first and second, and second and third natural frequencies, respectively. Ten measurement samples and 10,000 predictions from the estimated parameter distributions by method (1) are shown.

The effect of using different propagation methods (Monte-Carlo simulation, mean-centred first-order propagation, or the asymptotic integral) is considered in Table 3 and Figs. 17–19. It is seen that in this case specifically there is little advantage gained by using the more computationally demanding approaches (Monte-Carlo simulation, and the asymptotic integral) over the mean-centred first-order perturbation technique.

5.2. *Case study 2: Finite-element model of a pin-jointed truss*

The finite-element model consisting of 20 planar rod elements, each having 2 degree-of-freedom at every node, is shown in Fig. 20. The elastic modulus, mass density and cross sectional area were assumed to take the values,

$$E = 70\ \mathrm{GPa}, \quad \rho = 2700\ \mathrm{kg/m^3}, \quad A = 0.03\ \mathrm{m^2}$$

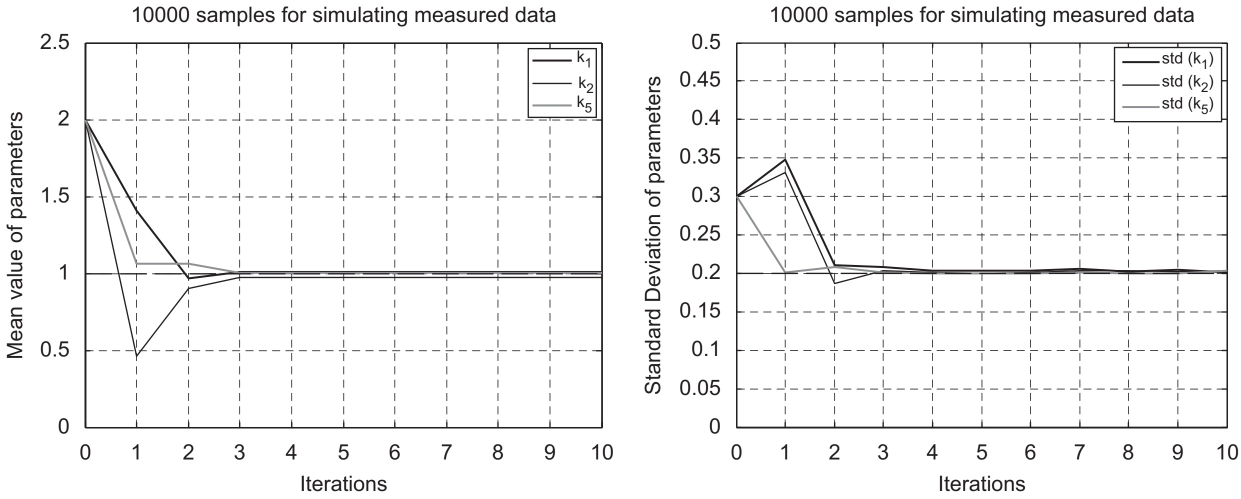

Fig. 5. Convergence of parameter estimates by method (1).

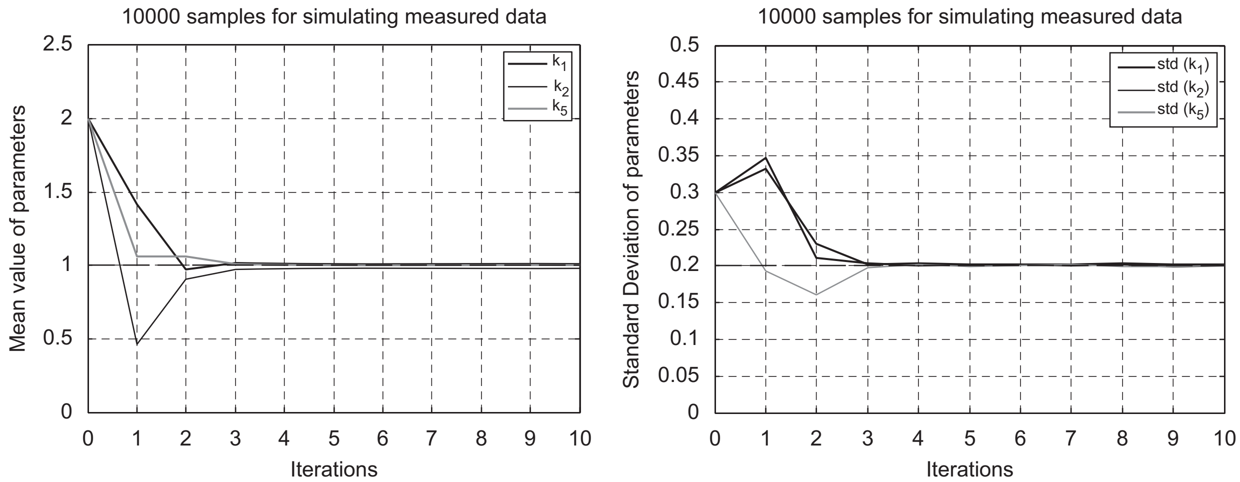

Fig. 6. Convergence of parameter estimates by method (2).

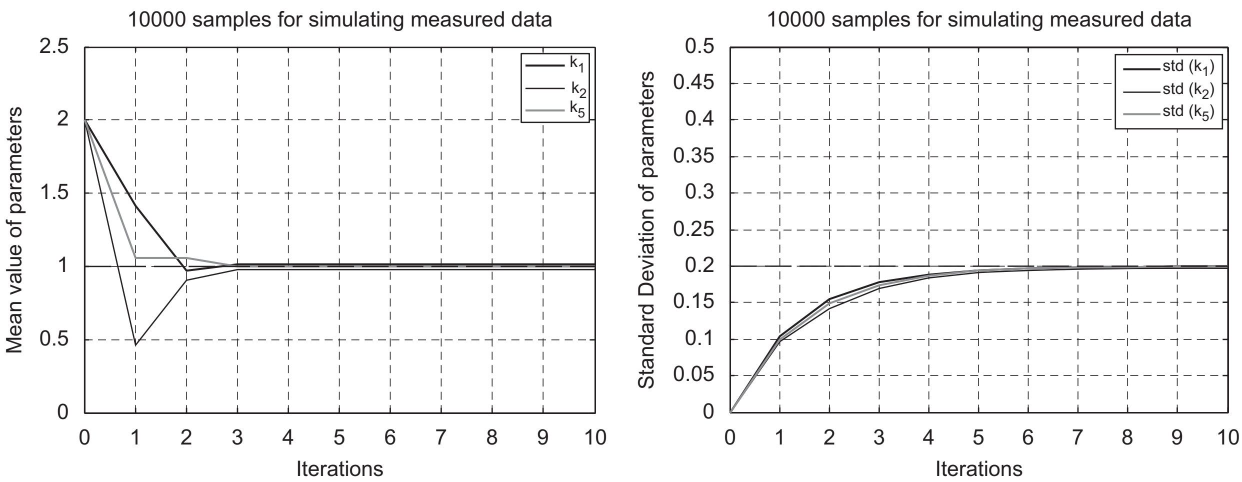

Fig. 7. Convergence of parameter estimates by method (3).

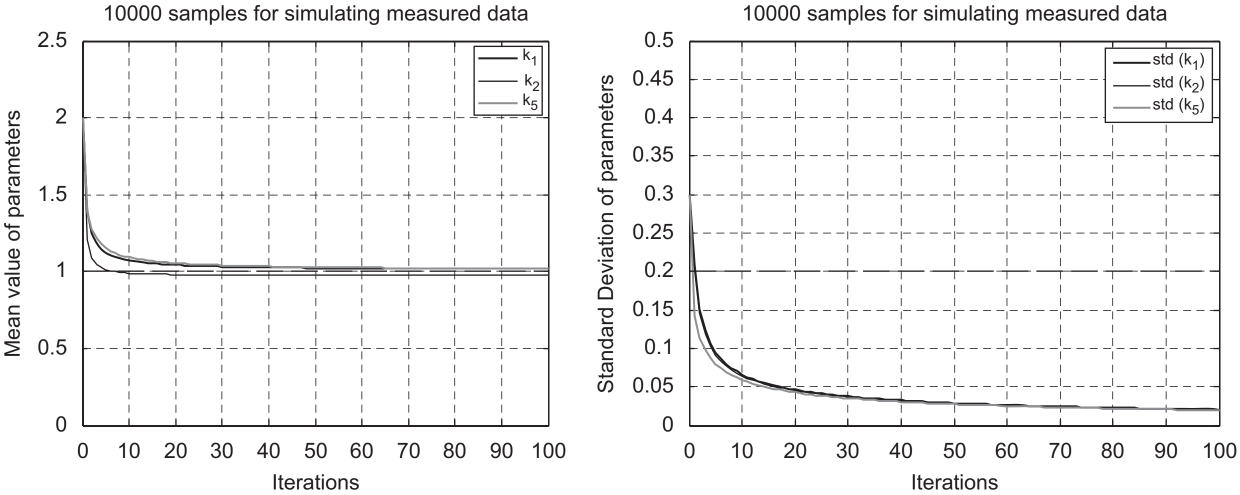

Fig. 8. Convergence of parameter estimates by method (4).

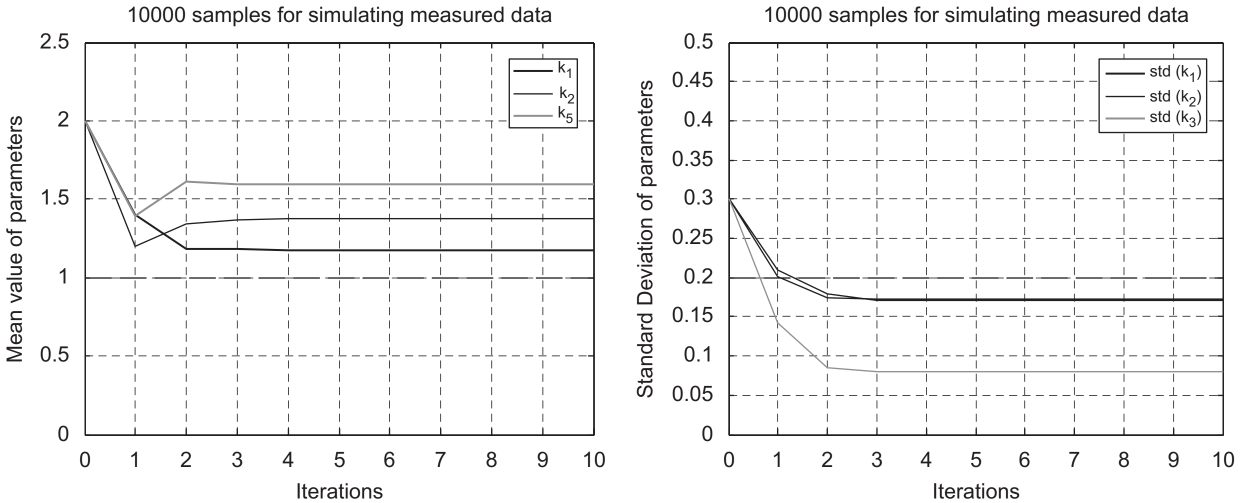

Fig. 9. Convergence of parameter estimates by method (5).

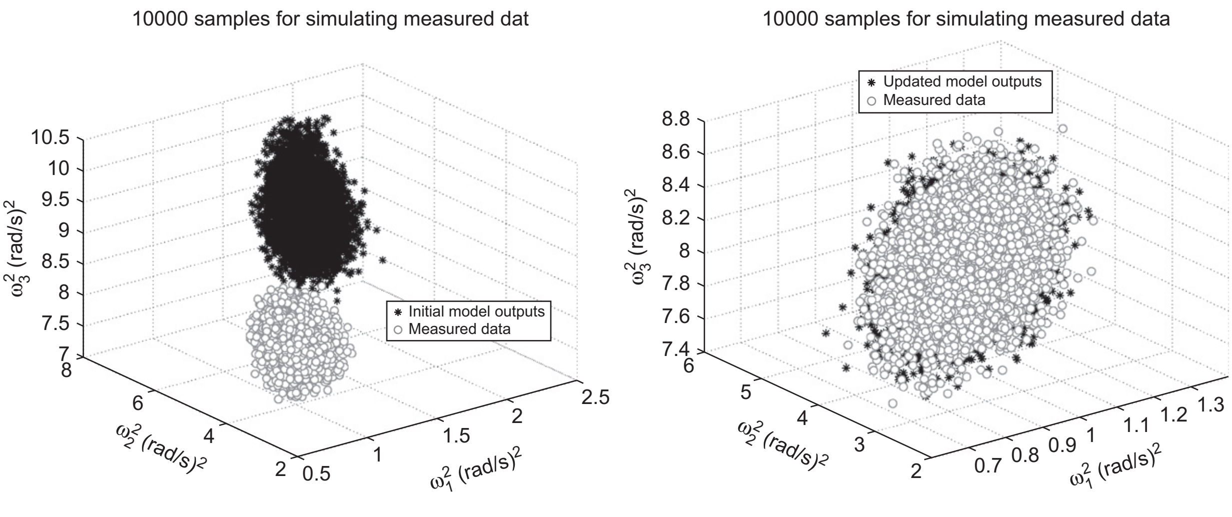

Fig. 10. Initial and updated scatter of predicted and measured data: identification using method (1) with 10,000 samples.

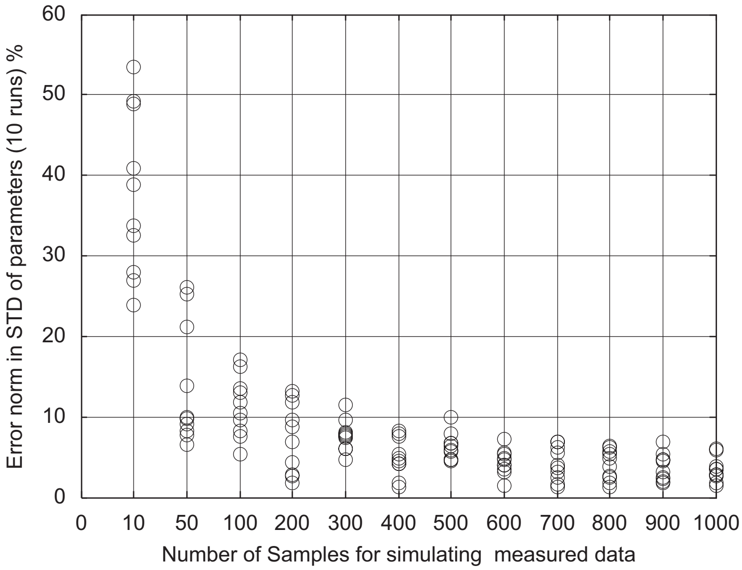

Fig. 11. Error norm for parameter standard deviations using different sample sizes each with 10 runs of the algorithm.

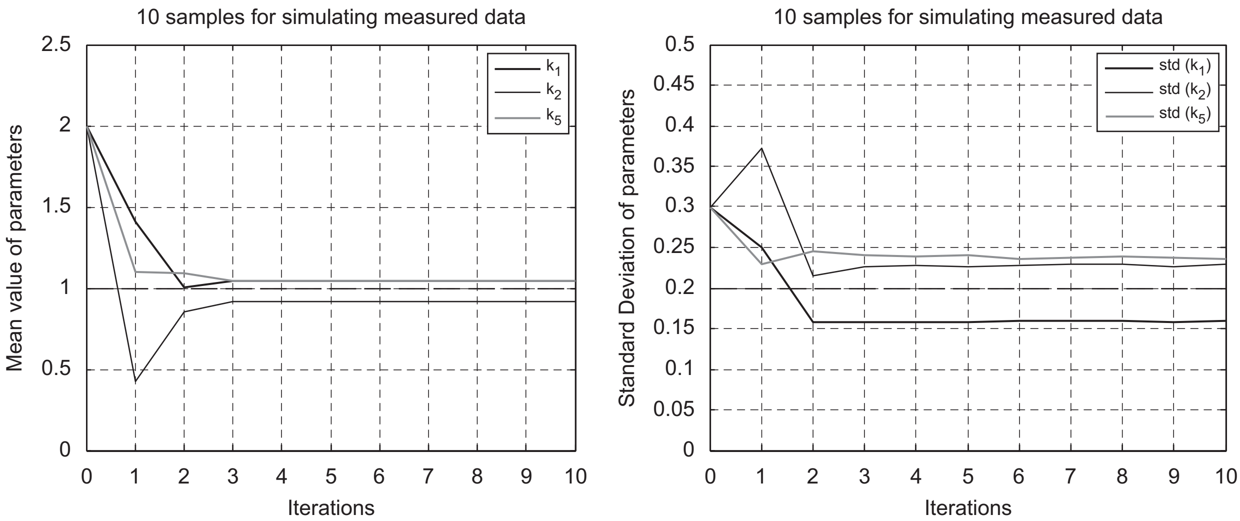

Fig. 12. Convergence of parameter estimates by method (1).

The diagonal elements in the finite-element model were represented by generic rod elements [22], having the generic stiffness matrices given by

$$\mathbf{K} = k_i \begin{bmatrix} 1 & -1 \\ -1 & 1 \end{bmatrix}$$

where k_i is generic parameter for the ith diagonal element. This parameter was a Gaussian random variable defined by

$$\mu_{k_i} = \frac{E_i A_i}{L_i} = 1.485 \times 10^8, \quad \frac{\sigma_{k_i}}{\mu_{k_i}} = 0.135, \quad i = 1, \ldots, 5$$

and the initial uncertain generic parameters were set as

$$\bar{k}_1 = 0.85\mu_{k_1}, \quad \bar{k}_2 = 1.05\mu_{k_2}, \quad \bar{k}_3 = 0.95\mu_{k_3}, \quad \bar{k}_4 = 0.90\mu_{k_4}, \quad \bar{k}_5 = 1.1\mu_{k_5}$$

$$\mathrm{COV}(k_1) = 2\frac{\sigma_{k_i}}{\mu_{k_i}},$$

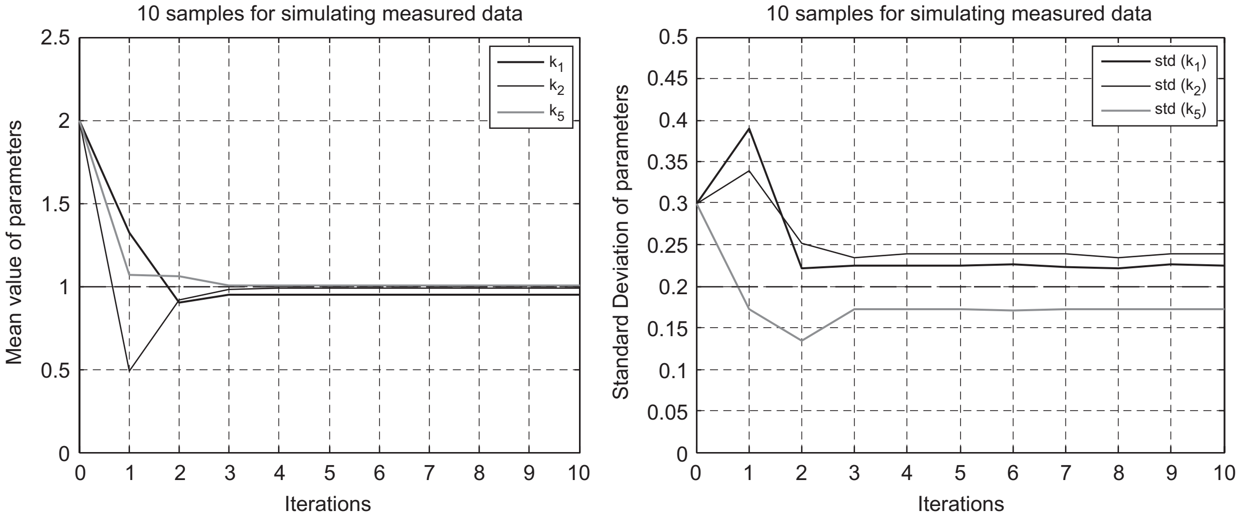

Fig. 13. Convergence of parameter estimates by method (2).

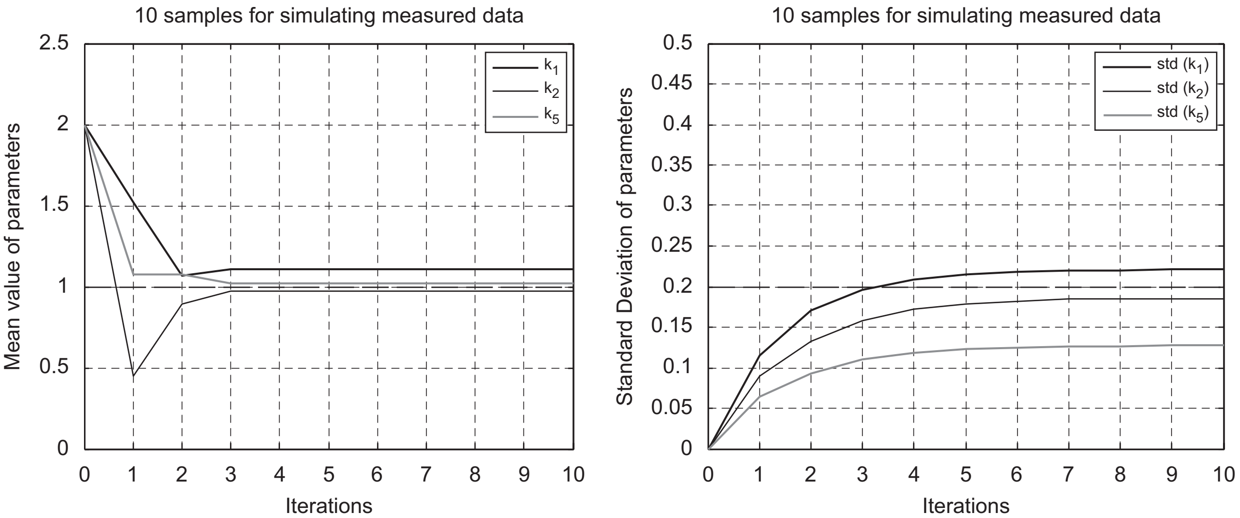

Fig. 14. Convergence of parameter estimates by method (3).

Table 2
Updating results by various methods (10 samples)

Parameters	Initial % error	% Error (1)	% Error (2)	% Error (3)
$\bar{k}_1$	100	4.53	−5.42	10.81
$\bar{k}_2$	100	−8.25	−1.52	1.73
$\bar{k}_5$	100	4.21	0.69	−2.86
S.D.(k_1)	50	−20.03	12.60	10.32
S.D.(k_2)	50	14.35	19.33	−7.26
S.D.(k_5)	50	17.65	−13.66	−36.44

where COV denotes the estimated coefficient of variation (ratio of the standard deviation to mean). The measurements consisted of the first four natural frequencies and four vertical displacements at nodes 5, 6, 11 and 12 for each of the first four modes, thereby generating 20 equations for updating five randomised parameters. Firstly, it was assumed that these equations do not contain any measurement noise. As expected, method (1) is capable of regenerating the exact simulated values of mean and COV for each of the randomised parameters as shown in Fig. 21. The weighting matrices were $\mathbf{W}_1 = \mathbf{I}$ and $\mathbf{W}_2 = \mathbf{0}$.

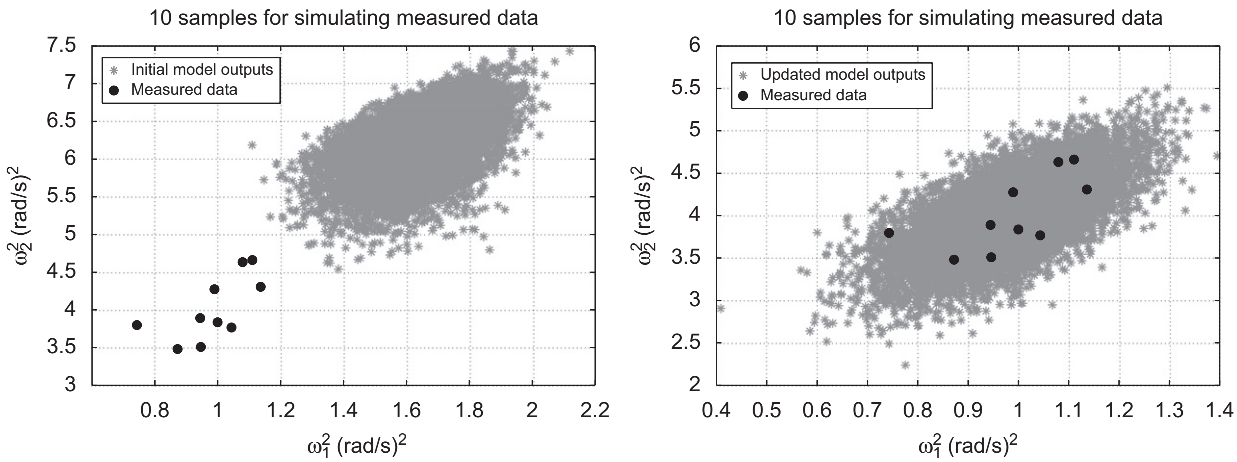

Fig. 15. Initial and updated scatter of predicted data (10,000 points) based upon 10 measurement samples: identification by method (1).

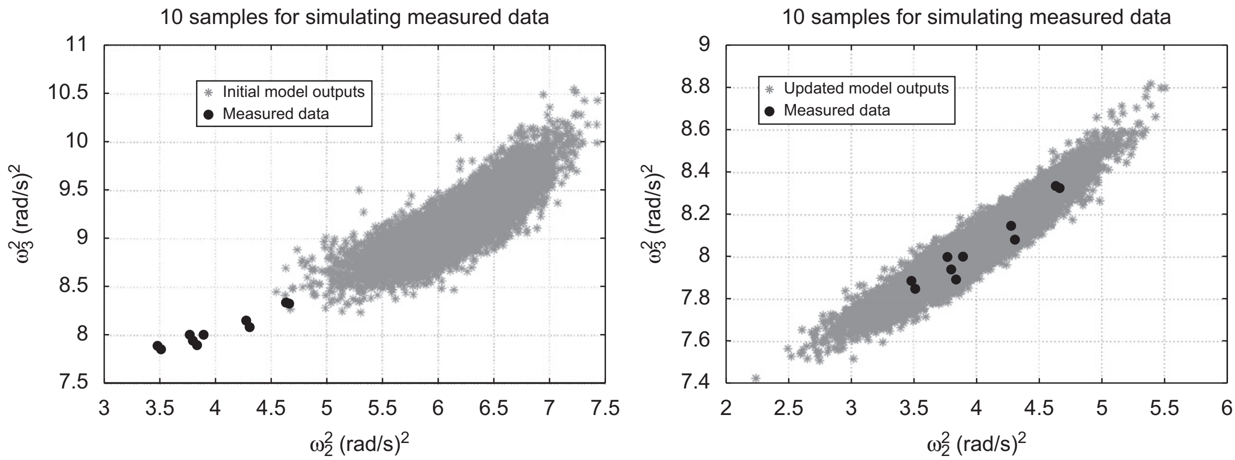

Fig. 16. Initial and updated scatter of predicted data (10,000 points) based upon 10 measurement samples: identification by method (1).

Table 3
Results by different propagation methods for evaluating covariance matrices (measured data were simulated by using just one set of 10 samples)

Parameter	Initial error (%)	Monte Carlo (%)	Perturbation (%)	Asymptotic (%)
$\bar{k}_1$	100	−3.72	−3.71	−2.47
$\bar{k}_2$	100	−1.49	−1.49	−3.13
$\bar{k}_5$	100	20.20	20.20	16.22
S.D.(k_1)	50	−19.99	−22.66	−20.72
S.D.(k_2)	50	−21.48	−24.85	−21.81
S.D.(k_5)	50	6.57	5.70	6.04

Method (1) was again applied, with and without regularisation, when 1% measurement noise with zero-mean Gaussian distribution was added to the measured data. Considerable errors were found in the estimated distribution when $\mathbf{W}_1 = \mathbf{I}$ and $\mathbf{W}_2 = \mathbf{0}$ as shown in Fig. 22. Regularisation was then applied with the regularisation parameter $\lambda = 0.001$ determined from the L-curve in Fig. 23. As can be seen from Fig. 24, the estimated distribution was greatly improved by the regularisation. The standard deviations were affected more by the presence of the noise than were the estimated means.

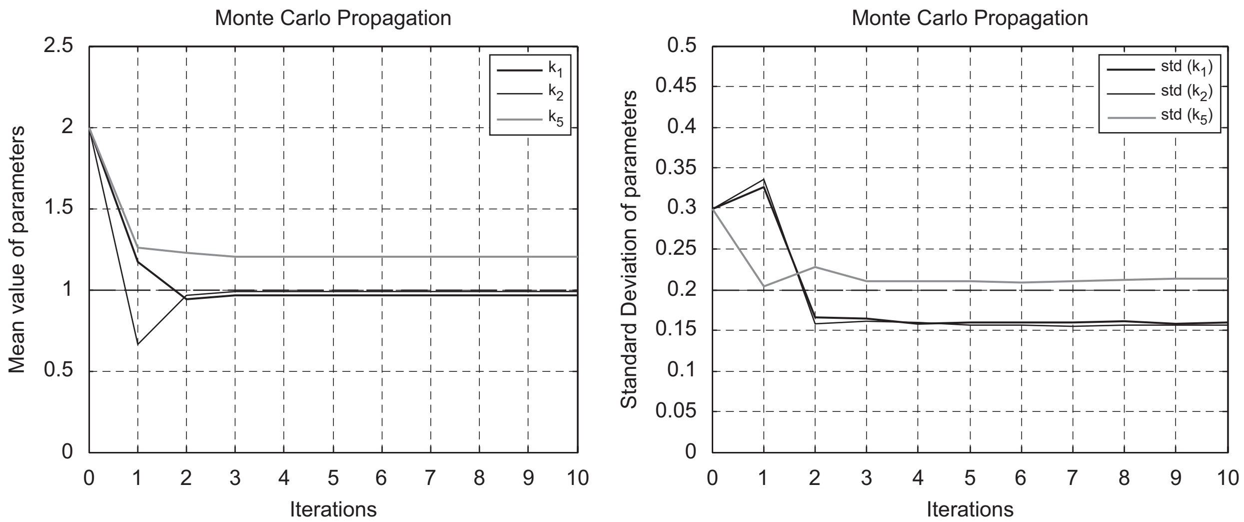

Fig. 17. Convergence of parameter estimates by method (1) using Monte-Carlo simulation.

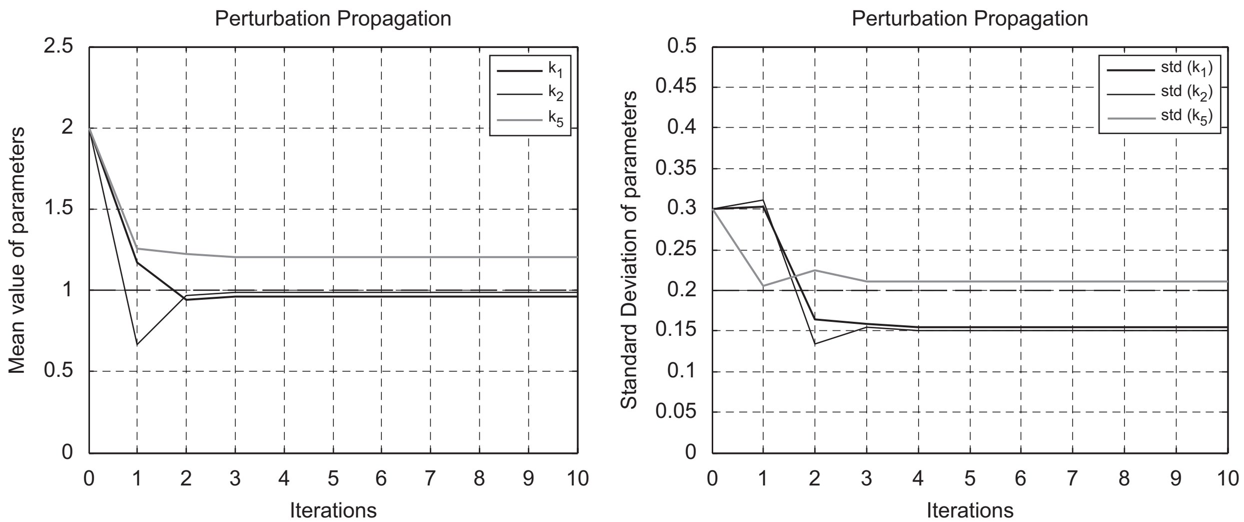

Fig. 18. Convergence of parameter estimates by method (1) using mean-centred first-order perturbation.

6. Experimental case study: Aluminium plates with random thicknesses

Ten aluminium plates were prepared so that a contrived distribution of thicknesses, close to Gaussian, was obtained by machining. Care was taken to try to obtain a constant thickness for each plate. This was not achieved perfectly and the thickness variations were measured using a long-jaw micrometer at 4×14 points as shown for example in Fig. 25. The distribution of nominal thicknesses is shown in Fig. 26. The mean value of the thicknesses was 3.975 mm with a standard deviation of 0.163 mm. In the experimental set up free boundary conditions were used to avoid the introduction of other uncertainties due to clamping or pinning at the edges of the plates. All 10 plates had the same overall dimensions, length 0.4 m and width 0.1 m. A hammer test was carried out using four uniaxial fixed accelerometers. Fig. 27 shows the excitation point, marked 'F', and the positions of four accelerometers, marked 'A', 'B', 'C' and 'D'. The mass of each accelerometer was 2 grams represented by lumped masses in the finite-element model. The first 10 measured natural frequencies of all 10 plates are given in Tables 4 and 5.

The thickness of the plates was parameterised in four regions as shown in Fig. 28 and a finite-element model was constructed consisting of 40×10 four-noded plate elements. The first six measured natural frequencies were used for stochastic model updating by method (1). A regularisation parameter, $\lambda = 1 \times 10^{10}$, was found from an L-curve. Fig. 29

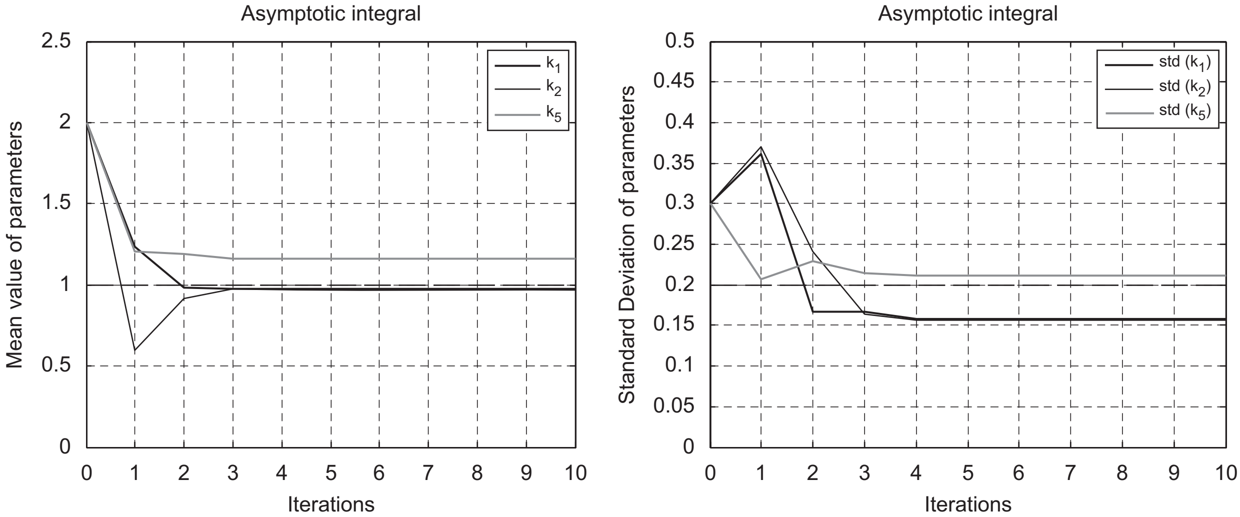

Fig. 19. Convergence of parameter estimates by method (1) using the asymptotic integral.

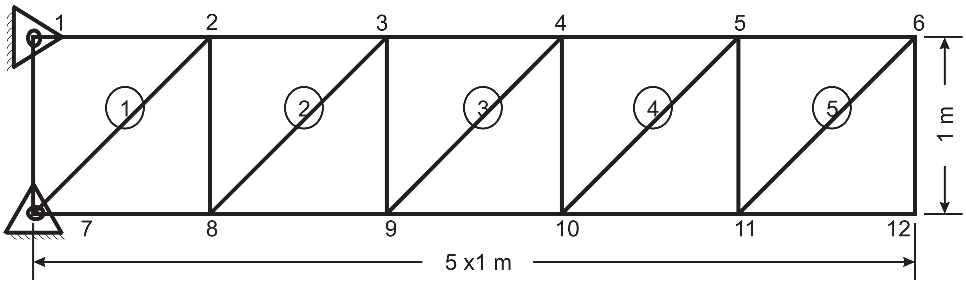

Fig. 20. FE model of pin-jointed truss.

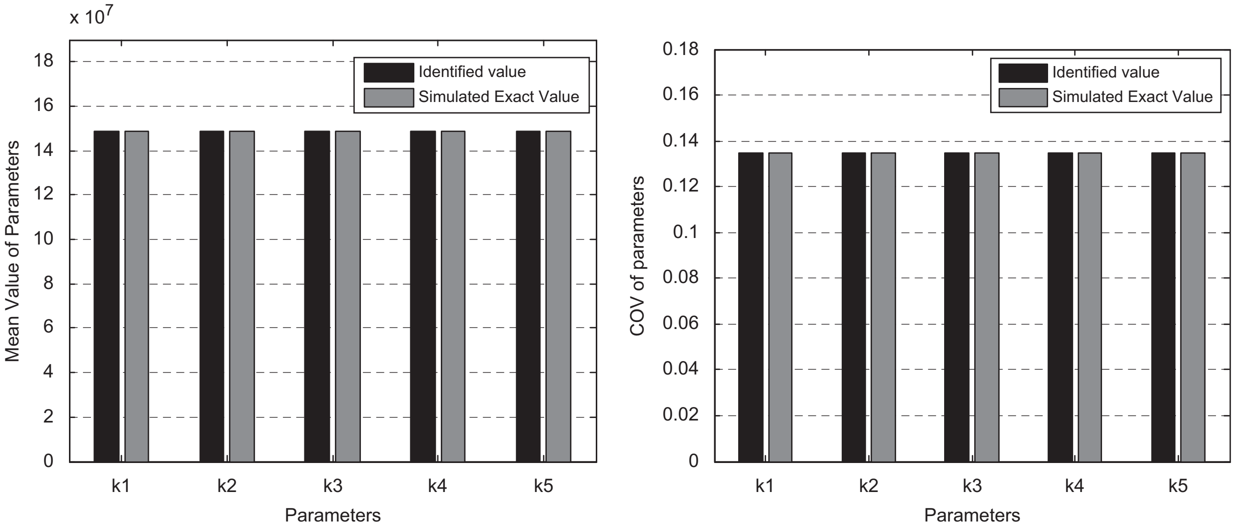

Fig. 21. Identified parameters—zero noise.

shows convergence of the mean values and COV for the four parameters. The initial mean and standard deviation of all four parameters were taken to be, $\bar{t}_i = 4$ mm, $\mathrm{S.D.}(t_i) = 0.8$ mm, $i = 1, \ldots, 4$. The initial mean value was chosen to be close to the true mean while the initial standard deviation was deliberately overestimated to represent a realistic stochastic model updating problem where little is known other than an approximation to the mean value.

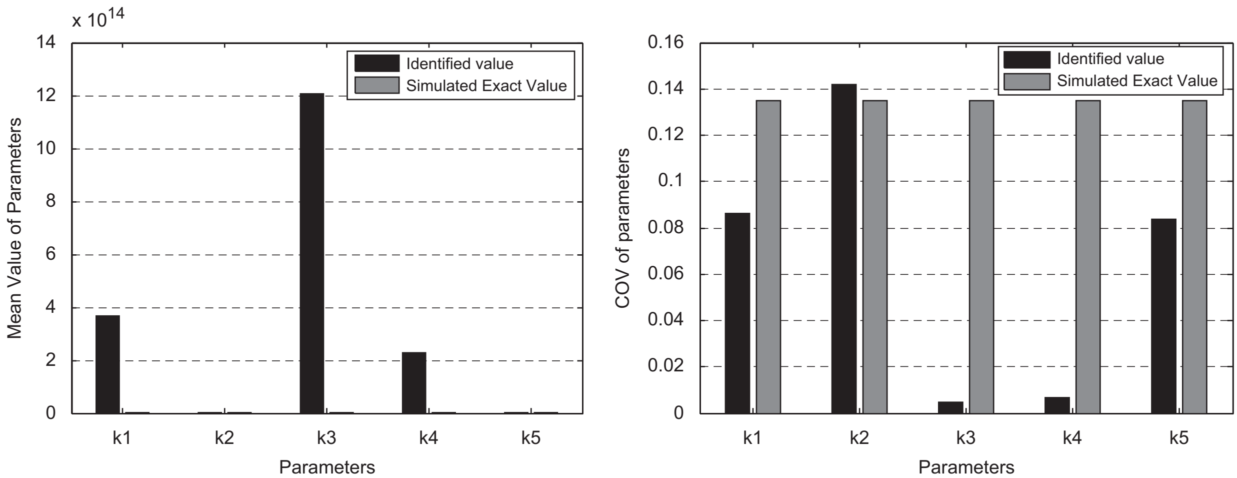

Fig. 22. Identified parameters with 1% measurement noise and $\mathbf{W}_1 = \mathbf{I}$, $\mathbf{W}_2 = \mathbf{0}$.

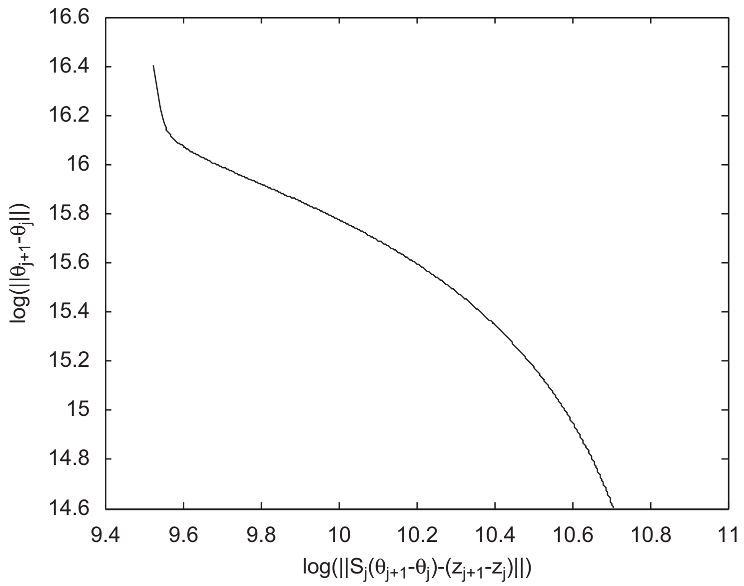

Fig. 23. L-curve.

The updated and measured means and standard deviations of the plate thicknesses are given in Table 6. These results are not in exact agreement but do show a considerable improvement in the thickness distributions when updated. It can be seen that the initial values of the means were chosen to be extremely close to the measured mean values. Small changes are observed in Table 6 after updating, away from the measured values obtained from averaged micrometer measurements at discrete points. The convergence of the standard deviations (shown in Table 6) from a considerable initial error is a much more significant result, demonstrating very clearly how well the method performs in converging the distribution of updating parameters upon the collection of measured thickness values. Of course, the measured standard deviations are likely to be less accurate than the measured means.

The means and standard deviations of the first six measured natural frequencies were used in updating, whereas 10 modes were measured in total. It is seen from Tables 7 and 8 that not only are the first six natural frequency distributions improved by updating but also the 7th–10th natural frequency predictions (mean and standard deviations) are equally improved. This provides a good demonstration of the validity of the updated statistical model.

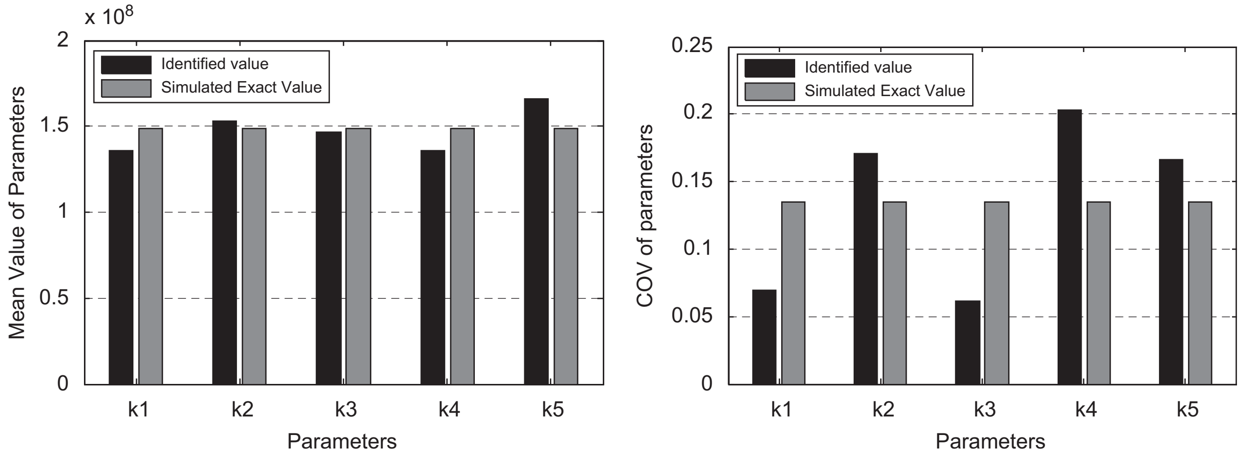

Fig. 24. Identified parameters 1% measurement noise and $\mathbf{W}_1 = \mathbf{I}$, $\mathbf{W}_2 = \lambda\mathbf{I}$.

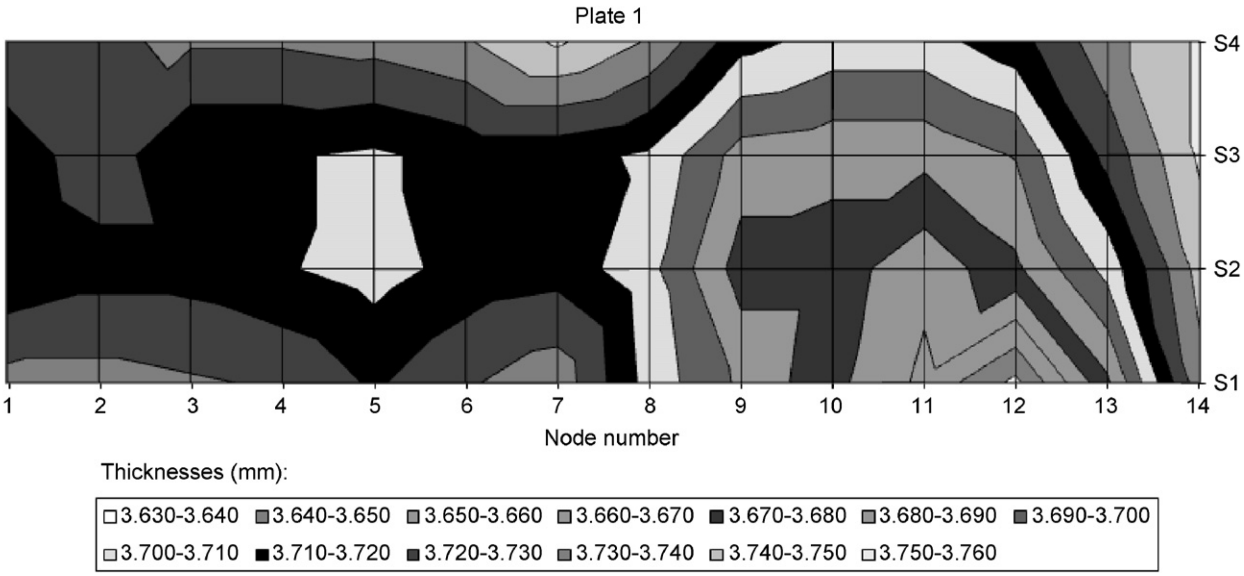

Fig. 25. Measured thickness of plate 1.

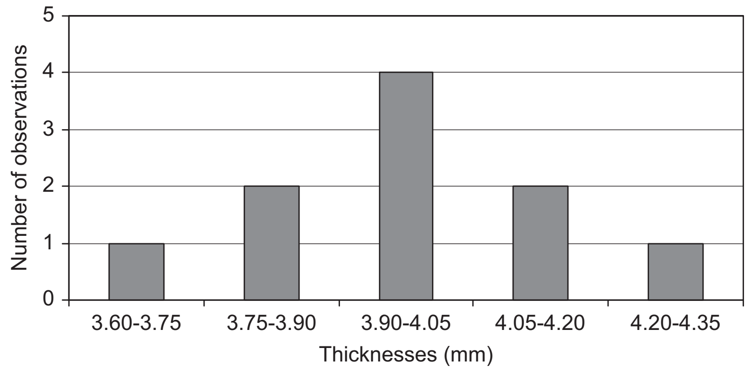

Fig. 26. Distribution of plate thicknesses.

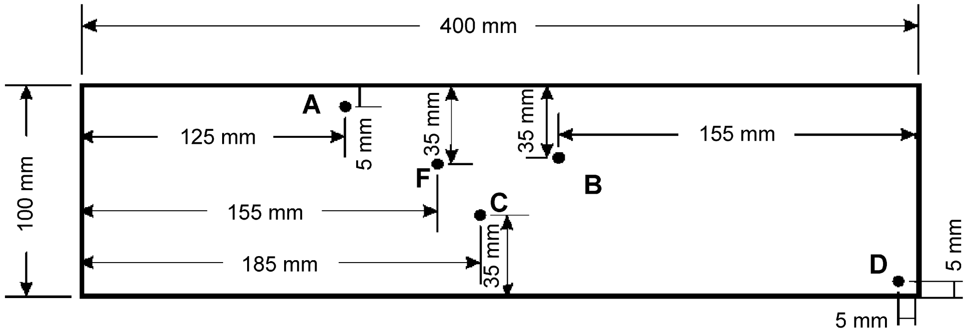

Fig. 27. Arrangement of accelerometers (A, B, C, D) and excitation point (F).

Table 4
The first five measured natural frequencies (Hz) for the 10 plates

Plate no.	Mode no.				
	1	2	3	4	5
1	119.774	284.283	331.970	589.404	656.359
2	121.615	291.922	337.186	605.160	665.854
3	123.156	291.440	340.184	602.603	673.357
4	128.048	298.163	355.210	620.139	700.798
5	128.533	303.809	357.110	630.809	704.505
6	128.596	301.010	361.488	635.533	713.207
7	129.796	311.726	361.114	646.765	712.792
8	135.058	315.393	374.368	653.584	738.395
9	134.478	312.215	374.406	649.130	737.256
10	138.141	321.812	382.932	667.203	755.189
Mean	128.720	303.177	357.597	630.033	705.771
S.D.	6.011	12.032	17.048	25.235	32.854

Table 5
The 6th to 10th measured natural frequencies (Hz) for 10 plates

Plate no.	Mode no.				
	6	7	8	9	10
1	932.576	1091.603	1343.097	1628.879	1825.215
2	953.666	1106.861	1372.890	1650.395	1860.225
3	955.515	1119.445	1376.298	1669.899	1868.071
4	980.403	1165.177	1414.181	1736.714	1924.260
5	995.188	1169.660	1433.020	1743.750	1946.155
6	999.248	1184.455	1440.134	1765.415	1957.581
7	1019.052	1184.608	1467.366	1766.361	1987.556
8	1031.837	1225.375	1487.512	1825.602	2021.640
9	1023.229	1224.420	1479.268	1824.121	2013.354
10	1053.974	1253.610	1519.011	1866.665	2031.377
Mean	994.469	1172.521	1433.278	1747.780	1943.543
S.D.	38.877	53.840	56.771	79.232	72.908

7. Conclusions

Two versions of a perturbation approach to the stochastic model updating problem, with test-structure variability, are developed. Distributions of predicted modal responses (natural frequencies and mode shapes) are converged upon measured distributions, resulting in estimates of the first two statistical moments of the randomised updating parameters.

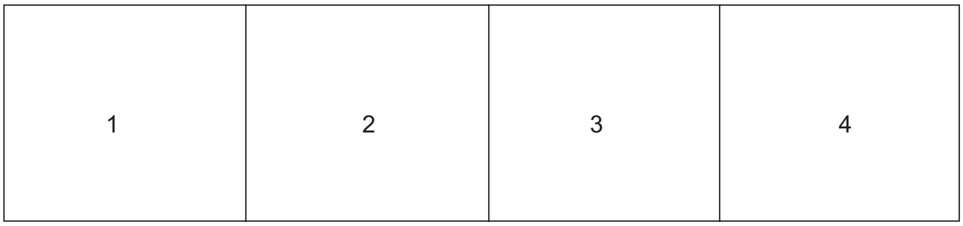

Fig. 28. Parameterisation into four regions of plate thickness.

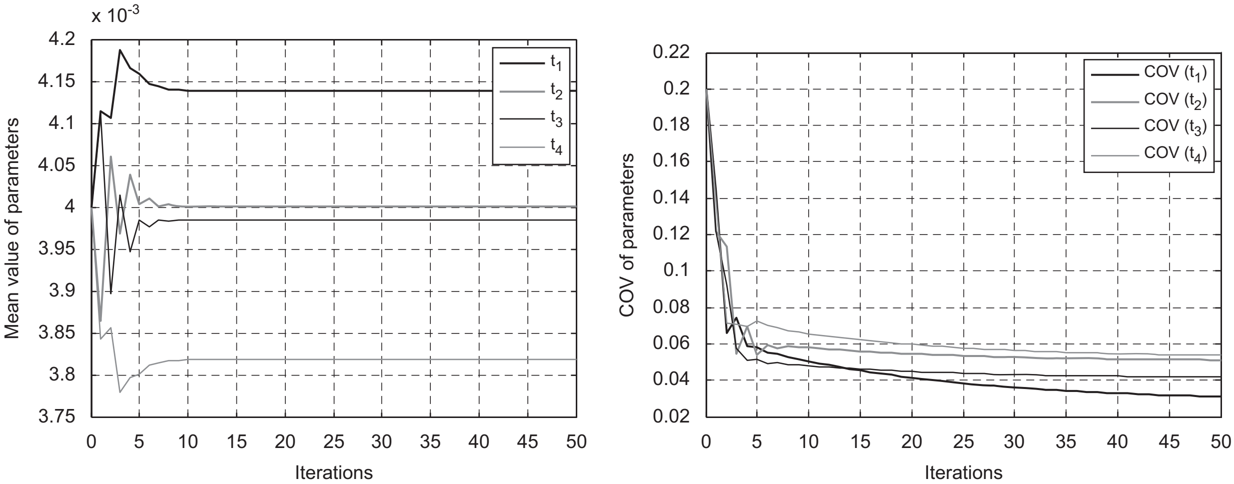

Fig. 29. Convergence of parameter estimates.

Table 6
Measured, initial and updated mean and standard deviation of parameters

	Measured parameters	Initial parameters	Updated parameters	Initial FE % error	Updated FE % error
$\bar{t}_1$(mm)	3.978	4.000	4.140	0.553	4.072
S.D.(t_1) (mm)	0.159	0.800	0.129	403.145	−18.868
$\bar{t}_2$(mm)	3.969	4.000	4.002	0.781	0.831
S.D.(t_2) (mm)	0.161	0.800	0.204	396.894	26.708
$\bar{t}_3$(mm)	3.982	4.000	3.986	0.452	0.100
S.D.(t_3) (mm)	0.164	0.800	0.166	387.805	1.219
$\bar{t}_4$(mm)	3.981	4.000	3.820	0.477	−4.044
S.D.(t_4) (mm)	0.167	0.800	0.206	379.042	23.353

Table 7
Measured, initial and updated mean natural frequencies

	Measured (Hz)	Initial FE (Hz)	Updated FE (Hz)	Initial FE % error	Updated FE % error
Mode (1)	128.720	128.321	128.111	−0.310	−0.473
Mode (2)	303.177	307.147	306.339	1.310	1.043
Mode (3)	357.597	356.645	355.185	−0.266	−0.675
Mode (4)	630.033	637.433	633.188	1.175	0.501
Mode (5)	705.771	705.467	701.777	−0.043	−0.566
Mode (6)	994.469	1002.229	996.865	0.780	0.241
Mode (7)	1172.521	1173.395	1169.087	0.075	−0.293
Mode (8)	1433.278	1444.018	1435.848	0.750	0.179
Mode (9)	1747.780	1748.977	1743.491	0.069	−0.245
Mode (10)	1943.543	1952.882	1935.851	0.481	−0.396

Table 8
Measured, initial and updated S.D. of natural frequencies

	Measured (Hz)	Initial FE (Hz)	Updated FE (Hz)	Initial FE % error	Updated FE % error
Mode (1)	6.011	20.943	5.750	248.411	−4.342
Mode (2)	12.032	47.385	13.777	293.825	14.503
Mode (3)	17.048	39.231	15.180	130.121	−10.957
Mode (4)	25.235	65.655	26.797	160.175	6.190
Mode (5)	32.854	71.379	28.644	117.261	−12.814
Mode (6)	38.877	108.445	40.166	178.944	3.316
Mode (7)	53.840	118.628	46.536	120.334	−13.566
Mode (8)	56.771	148.418	59.571	161.434	4.932
Mode (9)	79.232	177.244	70.452	123.702	−11.081
Mode (10)	72.908	202.753	83.427	178.094	14.428

Regularisation may be applied when the stochastic model updating equations are ill-conditioned. A computationally efficient solution, without any significant loss of accuracy, is obtained when the correlation between the randomised updating parameters and test data is omitted. The method is demonstrated in numerical simulations and also in an experiment carried out on a collection of rectangular plates with variable thickness.

Acknowledgement

H. Haddad Khodaparast wishes to acknowledge the support of EC Marie Curie Excellence Project ECERTA.

Appendix. Evaluation of covariances by the asymptotic integral method

Adhikari and Friswell [18] used the approximation (29) for evaluating the statistical moments of random eigenvalues. In the present study, we are concerned with integrals having the forms,

$$\begin{aligned}\mathrm{E}(z_i(\boldsymbol{\theta})z_k(\boldsymbol{\theta})) &= \int_{\Re^m} z_i(\boldsymbol{\theta})z_k(\boldsymbol{\theta})\mathrm{p}_\theta(\boldsymbol{\theta})\,\mathrm{d}\theta_1\,\mathrm{d}\theta_2\ldots\mathrm{d}\theta_m \\ &= \int_{\Re^m} \exp[-(\mathrm{L}(\boldsymbol{\theta}) - \ln(z_i(\boldsymbol{\theta})) - \ln(z_k(\boldsymbol{\theta})))]\,\mathrm{d}\theta_1\,\mathrm{d}\theta_2\ldots\mathrm{d}\theta_m, \quad i\neq k\end{aligned} \tag{A.1}$$

$$\begin{aligned}\mathrm{E}(\theta_i z_k(\boldsymbol{\theta})) &= \int_{\Re^m} \theta_i z_k(\boldsymbol{\theta})\mathrm{p}_\theta(\boldsymbol{\theta})\,\mathrm{d}\theta_1\,\mathrm{d}\theta_2\ldots\mathrm{d}\theta_m \\ &= \int_{\Re^m} \exp[-(\mathrm{L}(\boldsymbol{\theta}) - \ln(\theta_i) - \ln(z_k(\boldsymbol{\theta})))]\,\mathrm{d}\theta_1\,\mathrm{d}\theta_2\ldots\mathrm{d}\theta_m\end{aligned} \tag{A.2}$$

and

$$\mu_i = \int_{\Re^m} \theta_i \mathrm{p}_\theta(\boldsymbol{\theta})\,\mathrm{d}\theta_1\,\mathrm{d}\theta_2\ldots\mathrm{d}\theta_m = \int_{\Re^m} \exp[-(\mathrm{L}(\boldsymbol{\theta}) - \ln(\theta_i))]\,\mathrm{d}\theta_1\,\mathrm{d}\theta\ldots\mathrm{d}\theta_m \neq \bar{\theta}_i \tag{A.3}$$

the latter used in Eq. (32). It should be noted that $\mu_i \neq \theta_i$ since the integral includes all the probability density functions $\mathrm{p}_\theta(\boldsymbol{\theta})$. $\mathrm{L}(\boldsymbol{\theta})$ is the likelihood function.

In the case of the Gaussian distribution,

$$\mathrm{L}(\boldsymbol{\theta}) = \frac{m}{2}\ln(2\pi) + \frac{1}{2}\ln||\mathrm{Cov}(\boldsymbol{\theta},\boldsymbol{\theta})|| + \frac{1}{2}(\boldsymbol{\theta} - \bar{\boldsymbol{\theta}})^T(\mathrm{Cov}(\boldsymbol{\theta},\boldsymbol{\theta}))^{-1}(\boldsymbol{\theta} - \bar{\boldsymbol{\theta}}) \tag{A.4}$$

and the integrals (A.1)–(A.3) may be determined as follows:

1. Eq. (A.1)

$$\mathrm{E}(z_i(\boldsymbol{\theta})z_k(\boldsymbol{\theta})) \approx z_i(\boldsymbol{\varphi})z_k(\boldsymbol{\varphi})\exp\left\{-\frac{1}{2}(\boldsymbol{\varphi} - \bar{\boldsymbol{\theta}})^T(\mathrm{Cov}(\boldsymbol{\theta},\boldsymbol{\theta}))^{-1}(\boldsymbol{\varphi} - \bar{\boldsymbol{\theta}})\right\}||\mathbf{I} + \tilde{\mathbf{D}}_f(\boldsymbol{\varphi})||^{-1/2} \tag{A.5}$$

where

$$\begin{aligned}\tilde{\mathbf{D}}_f(\boldsymbol{\varphi}) = {} & \frac{1}{z_i^2(\boldsymbol{\varphi})}\mathrm{Cov}(\boldsymbol{\theta},\boldsymbol{\theta})\mathbf{d}_{z_i}(\boldsymbol{\varphi})\cdot\mathbf{d}_{z_i}(\boldsymbol{\varphi})^T + \frac{1}{z_k^2(\boldsymbol{\varphi})}\mathrm{Cov}(\boldsymbol{\theta},\boldsymbol{\theta})\mathbf{d}_{z_k}(\boldsymbol{\varphi})\cdot\mathbf{d}_{z_k}(\boldsymbol{\varphi})^T \\ & - \frac{1}{z_i(\boldsymbol{\varphi})}\mathrm{Cov}(\boldsymbol{\theta},\boldsymbol{\theta})\mathbf{D}_{z_i}(\boldsymbol{\varphi}) - \frac{1}{z_k(\boldsymbol{\varphi})}\mathrm{Cov}(\boldsymbol{\theta},\boldsymbol{\theta})\mathbf{D}_{z_k}(\boldsymbol{\varphi})\end{aligned} \tag{A.6}$$

and $\boldsymbol{\varphi}$ is found by solving the following equation numerically,

$$\boldsymbol{\varphi} = \bar{\boldsymbol{\theta}} + \frac{1}{z_i(\boldsymbol{\varphi})}\mathrm{Cov}(\boldsymbol{\theta},\boldsymbol{\theta})\mathbf{d}_{z_i}(\boldsymbol{\varphi}) + \frac{1}{z_k(\boldsymbol{\varphi})}\mathrm{Cov}(\boldsymbol{\theta},\boldsymbol{\theta})\mathbf{d}_{z_k}(\boldsymbol{\varphi}) \tag{A.7}$$

with $\mathbf{d}_{z_i}(\boldsymbol{\varphi})$, the gradient vector of the ith output parameter, z_i, with respect to system parameters, evaluated at the optimal point $\boldsymbol{\theta} = \boldsymbol{\varphi}$.

2. Eq. (A.2)

$$\mathrm{E}(\theta_i z_k(\boldsymbol{\theta})) \approx \varphi_i z_k(\boldsymbol{\varphi})\exp\left\{-\frac{1}{2}(\boldsymbol{\varphi}-\bar{\boldsymbol{\theta}})^T(\mathrm{Cov}(\boldsymbol{\theta},\boldsymbol{\theta}))^{-1}(\boldsymbol{\varphi}-\bar{\boldsymbol{\theta}})\right\}||\mathbf{I}+\widetilde{\mathbf{D}}_f(\boldsymbol{\varphi})||^{-1/2} \tag{A.8}$$

where

$$\widetilde{\mathbf{D}}_f(\boldsymbol{\varphi}) = (\boldsymbol{\varphi}-\bar{\boldsymbol{\theta}}-\mathrm{Cov}(\boldsymbol{\theta},\boldsymbol{\theta})\boldsymbol{\zeta})(\boldsymbol{\varphi}-\bar{\boldsymbol{\theta}}-\mathrm{Cov}(\boldsymbol{\theta},\boldsymbol{\theta})\boldsymbol{\zeta})^T(\mathrm{Cov}(\boldsymbol{\theta},\boldsymbol{\theta}))^{-1} - \frac{1}{z_k(\boldsymbol{\varphi})}\mathbf{D}_{z_k}(\boldsymbol{\varphi}) - \mathrm{Cov}(\boldsymbol{\theta},\boldsymbol{\theta})\times\boldsymbol{\Xi} \tag{A.9}$$

and $\boldsymbol{\varphi}$ is found by numerical solution of

$$\boldsymbol{\varphi} = \bar{\boldsymbol{\theta}} + \frac{1}{z_i(\boldsymbol{\varphi})}\mathrm{Cov}(\boldsymbol{\theta},\boldsymbol{\theta})\mathbf{d}_{z_i}(\boldsymbol{\varphi}) + \mathrm{Cov}(\boldsymbol{\theta},\boldsymbol{\theta})\boldsymbol{\zeta} \tag{A.10}$$

Also,

$$\boldsymbol{\zeta} = [\zeta_1,\zeta_2,\ldots,\zeta_j,\ldots\zeta_m]^T;\quad \zeta_j = \begin{cases}\frac{1}{\varphi_i} & \text{if } j=i\\ 0 & \text{if } j\neq i\end{cases}\quad i=1,\ldots,m \tag{A.11}$$

and,

$$\boldsymbol{\Xi} = \mathrm{diag}(\boldsymbol{\psi})\quad\text{and}\quad \boldsymbol{\psi} = [\psi_1,\psi_2,\ldots,\psi_j,\ldots,\psi_m]^T;\quad \psi_j = \begin{cases}-\frac{1}{\varphi_i^2} & \text{if } j=i\\ 0 & \text{if } j\neq i\end{cases} \tag{A.12}$$

3. Eq. (A.3)

$$\mu_i \approx \varphi_i\ \exp\left\{-\frac{1}{2}(\boldsymbol{\varphi}-\bar{\boldsymbol{\theta}})^T(\mathrm{Cov}(\boldsymbol{\theta},\boldsymbol{\theta}))^{-1}(\boldsymbol{\varphi}-\bar{\boldsymbol{\theta}})\right\}||\mathbf{I}+\widetilde{\mathbf{D}}_f(\boldsymbol{\varphi})||^{-1/2}, \tag{A.13}$$

where

$$\widetilde{\mathbf{D}}_f(\boldsymbol{\varphi}) = -\mathrm{Cov}(\boldsymbol{\theta},\boldsymbol{\theta})\boldsymbol{\Xi} \tag{A.14}$$

and $\boldsymbol{\varphi}$ is found from the numerical solution of

$$\boldsymbol{\varphi} = \bar{\boldsymbol{\theta}} + \mathrm{Cov}(\boldsymbol{\theta},\boldsymbol{\theta})\boldsymbol{\zeta} \tag{A.15}$$

The asymptotic integral method is described in detail by Adhikari and Friswell [18]. As can be seen from Eq. (31) , the diagonal terms of $\mathrm{Cov}(\mathbf{z},\mathbf{z})$ require that $E(z_k(\theta))$ and $E(z_k^2(\boldsymbol{\theta}))$ are evaluated as follows [18]:

$$\mathrm{E}(z_k^r(\boldsymbol{\theta})) \approx (2\pi)^{m/2} z_k^r(\boldsymbol{\varphi})\exp\left\{-\frac{1}{2}(\boldsymbol{\varphi}-\bar{\boldsymbol{\theta}})^T(\mathrm{Cov}(\boldsymbol{\theta},\boldsymbol{\theta}))^{-1}(\boldsymbol{\varphi}-\bar{\boldsymbol{\theta}})\right\}||\mathbf{I}+\widetilde{\mathbf{D}}_f(\boldsymbol{\varphi})||^{-1/2}\quad r=1,2 \tag{A.16}$$

where

$$\widetilde{\mathbf{D}}_f(\boldsymbol{\varphi}) = \frac{1}{r}(\boldsymbol{\varphi}-\bar{\boldsymbol{\theta}})(\boldsymbol{\varphi}-\bar{\boldsymbol{\theta}})^T(\mathrm{Cov}(\boldsymbol{\theta},\boldsymbol{\theta}))^{-1} - \frac{r}{z_k(\boldsymbol{\varphi})}\mathrm{Cov}(\boldsymbol{\theta},\boldsymbol{\theta})\mathbf{D}_{z_k}(\boldsymbol{\varphi}) \tag{A.17}$$

and $\boldsymbol{\varphi}$ may be obtained according to

$$\boldsymbol{\varphi} = \bar{\boldsymbol{\theta}} + \frac{r}{z_k(\boldsymbol{\varphi})}\mathrm{Cov}(\boldsymbol{\theta},\boldsymbol{\theta})\mathbf{d}_{z_k}(\boldsymbol{\varphi}) \tag{A18}$$

References

[1] J.E. Mottershead, M.I. Friswell, Model updating in structural dynamics: a survey, Journal of Sound and Vibration 167 (2) (1993) 347–375.
[2] M.I. Friswell, J.E. Mottershead, Finite Element Model Updating in Structural Dynamics, Kluwer Academic Press, Dordrecht, 1995.
[3] C. Mares, J.E. Mottershead, M.I. Friswell, Stochastic model updating: Part 1—Theory and simulated example, Mechanical Systems and Signal Processing 20 (2006) 1674–1695.
[4] J.E. Mottershead, C. Mares, M.I. Friswell, Stochastic model updating: Part 2—Application to a set of physical structures, Mechanical Systems and Signal Processing 20 (2006) 2171–2185.
[5] Y. Xia, H. Hao, J.M.W. Brownjohn, P.Q. Xia, Damage identification of structures with uncertain frequency and mode shape data, Earthquake Engineering and Structural Dynamics 31 (2002) 1053–1066.
[6] Y. Xia, H. Hao, Statistical damage identification of structures with frequency changes, Journal of Sound and Vibration 263 (2003) 853–870.

[7] X.G. Hua, Y.Q. Ni, Z.Q. Chen, J.M. Ko, An improved perturbation method for stochastic finite element model updating, International Journal for Numerical Methods in Engineering 73 (2008) 1845–1864.
[8] Y. Govers, M. Böswald, U. Füllekrug, D. Göge, M. Link, Analysis of sources and quantification of uncertainty in experimental modal data, in: International Conference on Noise and Vibration Engineering, ISMA2006, Katholieke Universiteit Leuven, 18–20 September 2006, Leuven, Belgium, 2006, pp. 4161–4173.
[9] D. Moens, D. Vandepitte, Recent advances in non-probabilistic approaches for non-deterministic dynamic finite element analysis, Archives of Computational Methods in Engineering 13 (3) (2006) 389–464.
[10] J.D. Collins, G.C. Hart, T.K. Hasselman, B. Kennedy, Statistical identification of structures, AIAA Journal 12 (2) (1974) 185–190.
[11] M.I. Friswell, The adjustment of structural parameters using a minimum variance estimator, Mechanical Systems and Signal Processing 3 (2) (1989) 143–155.
[12] J.L. Beck, L.S. Katafygiotis, Updating models and their uncertainties. I: Bayesian statistical framework, Journal of Engineering Mechanics 124 (4) (1998) 455–461.
[13] L.S. Katafygiotis, J.L. Beck, Updating models and their uncertainties. II: Model identifiability, Journal of Engineering Mechanics 124 (4) (1998) 463–467.
[14] G. Kerschen, J.C. Golinval, F.M. Hemez, Bayesian model screening for the identification of nonlinear mechanical structures, Journal of Vibration and Acoustics 125 (2003) 389–397.
[15] C. Mares, B. Dratz, J.E. Mottershead, M.I. Friswell, Model updating using Bayesian estimation, in: International Conference on Noise and Vibration Engineering, ISMA2006, Katholieke Universiteit Leuven, 18–20 September 2006, pp. 2607–2616.
[16] J.R. Fonseca, M.I. Friswell, J.E. Mottershead, A.W. Lees, Uncertainty identification by the maximum likelihood method, Journal of Sound and Vibration 288 (2005) 587–599.
[17] C. Papadimitriou, J.L. Beck, L.S. Katafygiotis, Asymptotic expansion for reliability and moments of uncertain systems, Journal of Engineering Mechanics 123 (12) (1997) 1219–1229.
[18] S. Adhikari, M.I. Friswell, Random matrix eigenvalue problems in structural dynamics, International Journal for Numerical Methods in Engineering 69 (2007) 562–591.
[19] F.M. Hemez, S.W. Doebling, M.C. Anderson, A brief tutorial on verification and validation, in: Proceedings of the 22nd International Modal Analysis Conference, Dearborn, USA, 2004.
[20] H. Ahmadian, J.E. Mottershead, M.I. Friswell, Regularisation methods for finite element model updating, Mechanical Systems and Signal Processing 12 (1998) 47–64.
[21] N. Bleistein, R.A. Handelsman, Asymptotic Expansions of Integrals, Holt, Rinehart and Winston, New York, USA, 1994.
[22] G.M. Gladwell, H. Ahmadian, Generic element matrices suitable for finite element updating, Mechanical Systems and Signal Processing 9 (1996) 601–614.